(2)

IDA DOCUMENT D-1197

STANDARD ATMOSPHERES FOR ENGAGEMENT MODELING

Ernest Bauer

June 1993

Prepared for
Ballistic Missile Defense Organization

INSTITUTE FOR DEFENSE ANALYSES
1801 N. Beauregard Street, Alexandria, Virginia 22311-1772

IDA Log No. HQ 92-42146

DEFINITIONS

IDA publishes the following documents to report the results of its work.

Reports

Reports are the most authoritative and most carefully considered products IDA publishes. They normally embody results of major projects which (a) have a direct bearing on decisions affecting major programs, (b) address issues of significant concern to the Executive Branch, the Congress and/or the public, or (c) address issues that have significant economic implications. IDA Reports are reviewed by outside panels of experts to ensure their high quality and relevance to the problems studied, and they are released by the President of IDA.

Group Reports

Group Reports record the findings and results of IDA established working groups and panels composed of senior individuals addressing major issues which otherwise would be the subject of an IDA Report. IDA Group Reports are reviewed by the senior individuals responsible for the project and others as selected by IDA to ensure their high quality and relevance to the problems studied, and are released by the President of IDA.

Papers

Papers, also authoritative and carefully considered products of IDA, address studies that are narrower in scope than those covered in Reports. IDA Papers are reviewed to ensure that they meet the high standards expected of refereed papers in professional journals or formal Agency reports.

Documents

IDA Documents are used for the convenience of the sponsors or the analysts (a) to record substantive work done in quick reaction studies, (b) to record the proceedings of conferences and meetings, (c) to make available preliminary and tentative results of analyses, (d) to record data developed in the course of an investigation, or (e) to forward information that is essentially unanalyzed and unevaluated. The review of IDA Documents is suited to their content and intended use.

The work reported in this document was conducted under contract MDA 903 89 C 0003 for the Department of Defense. The publication of this IDA document does not indicate endorsement by the Department of Defense, nor should the contents be construed as reflecting the official position of that Agency.

PAGES _____

ARE

MISSING

IN

ORIGINAL

DOCUMENT

REPORT DOCUMENTATION PAGE

Form Approved OMB No. 0704-0188

1. AGENCY USE ONLY *(Leave blank)*	2. REPORT DATE	3. REPORT TYPE AND DATES COVERED
	June 1993	Final--December 1991-November 1992

4. TITLE AND SUBTITLE

Standard Atmospheres for Engagement Modeling

5. FUNDING NUMBERS

C - MDA 903 89 C 0003

T- T-R2-597.12

6. AUTHOR(S)

Ernest Bauer

7. PERFORMING ORGANIZATION NAME(S) AND ADDRESS(ES)

Institute for Defense Analyses
1801 N. Beauregard St.
Alexandria, VA 22311-1772

8. PERFORMING ORGANIZATION REPORT NUMBER

IDA Document D-1197

9. SPONSORING/MONITORING AGENCY NAME(S) AND ADDRESS(ES)

BMDO
Washington, DC 20301-7100

10. SPONSORING/MONITORING AGENCY REPORT NUMBER

11. SUPPLEMENTARY NOTES

12a. DISTRIBUTION/AVAILABILITY STATEMENT

Approved for public release; distribution unlimited.

12b. DISTRIBUTION CODE

13. ABSTRACT *(Maximum 200 words)*

This document reviews the use of model atmospheres for Ballistic Missile Defense (BMD) engagement modeling. BMD engagement models simulate a ballistic missile attack from launch to interception. Model atmospheres are descriptions of atmospheric density and temperature as functions of altitude. However, BMD applications are not consistent in the choice of model atmosphere within a system application and, in fact, may employ more than one model atmosphere within an engagement model. The most widely used model atmospheres are the US-62 and US-76 models. These two differ significantly in the variable of solar activity. Thus, if engagement models run using both the US-62 and US-76 model atmospheres give the same result, the effect of the model atmosphere can probably be ruled out. We recommend that to measure the effects of atmospheric variability on a particular BMD application, engagement models be run using both the US-62 and US-76 model atmospheres. If the results differ, more detailed examination of the physics of the atmosphere for the problem under consideration may be called for.

14. SUBJECT TERMS	15. NUMBER OF PAGES
atmosphere, atmosphere models, atmospheric temperature, density profile, satellites, atmospheric density, rarefied atmosphere	69
	16. PRICE CODE

17. SECURITY CLASSIFICATION OF REPORT	18. SECURITY CLASSIFICATION OF THIS PAGE	19. SECURITY CLASSIFICATION OF ABSTRACT	20. LIMITATION OF ABSTRACT
UNCLASSIFIED	UNCLASSIFIED	UNCLASSIFIED	SAR

IDA DOCUMENT D-1197

STANDARD ATMOSPHERES FOR ENGAGEMENT MODELING

Ernest Bauer

June 1993

INSTITUTE FOR DEFENSE ANALYSES

Contract MDA 903 89 C 0003
Task T-R2-597.12

FOREWORD

In the early days of the Strategic Defense Initiative (SDI) it was necessary to adopt some kind of Model Atmosphere (i.e., a set of density and temperature values as a function of altitude) for engagement modeling.[1] The initial choice for the Threat Tape Generator (TTG) at the National Test Facility, Falcon AFB, Colorado, was the U.S. 1962 Standard Atmosphere, with zero density above 300 kft (91 km) and using a spherical model for the Earth. This was appropriate at the time (1986-88) but is not adequate for present (1992-93) requirements for ballistic missile targeting, tracking, and interception.

In March 1992 the SDIO [now Ballistic Missile Defense Organization (BMDO)] Environments Working Group (EWG) received an informal request to address the problem of a new standard atmosphere in light of the fact that there are now numerous engagement codes with different model atmospheres--and some level of standardization is urgently required. Causing minimum disruption to ongoing operations such as the TTG is also an important consideration. This document was prepared in response to both the EWG request and a generally perceived need to address the problem.

---

[1] The various model atmospheres differ at high altitudes (> 100 km) due to different levels of solar activity.

ACKNOWLEDGMENTS

Early discussions with Rex Finke and Peter Kysar of IDA, Greg Naidenko of Teledyne Brown, and Bill Riley, RDA/Logicon, were very helpful in defining the problem addressed. The document was reviewed by Russ Armstrong, MRC, Peter Kysar, IDA, Bill Riley, RDA/Logicon, and Edwin Townsley, IDA. These reviews have been outstanding, both in correcting errors in fact and emphasis and in making the document more relevant to the users.

ABSTRACT

This document reviews the use of model atmospheres for Ballistic Missile Defense (BMD) engagement modeling. BMD engagement models simulate a ballistic missile attack from launch to interception. Model atmospheres are descriptions of atmospheric density and temperature as functions of altitude. However, BMD applications are not consistent in the choice of model atmosphere within a system application and, in fact, may employ more than one model atmosphere within an engagement model. The most widely used model atmospheres are the US-62 and US-76 models. These two differ significantly in the variable of solar activity. Thus, if engagement models run using both the US-62 and US-76 model atmospheres give the same result, the effect of the model atmosphere can probably be ruled out. We recommend that to measure the effects of atmospheric variability on a particular BMD application, engagement models be run using both the US-62 and US-76 model atmospheres. If the results differ, more detailed examination of the physics of the atmosphere for the problem under consideration may be called for.

CONTENTS

FIGURES

TABLES

GLOSSARY

AAIAA	American Institute of Aeronautics and Astronautics
AGW	acoustic gravity waves
AMEM	an engagement code (developed by SAIC for USA SSDC)
ANSI	American National Standards Institute
Ap	geomagnetic activity index
ARDC	Air Research and Development Command
BMD	Ballistic Missile Defense
CIRA 65-Model 5/h8	CIRA model atmosphere (1965) representing average geomagnetic activity
CIRA	COSPAR International Reference Atmosphere
COSPAR	Committee on Space and Atmospheric Research
DEBRA	kinetic debris code
DNA	Defense Nuclear Agency
$F_{10.7}$	index of solar power flux density at 10.7-cm wavelength
FSU	Former Soviet Union
GPALS	Global Protection Against Limited Strikes
HiSEMM	USA-SSDC nuclear code
ICAO	International Civil Aviation Organization
ICBM	intercontinental ballistic missile
IGY	International Geophysical Year
INMD	Initial National Missile Defense
IRBM	intermediate range ballistic missile
ISTC	Integrated System Test Capability (BMD Simulation Code)

KIDD	kinetic debris code
MSIS	Mass Spectrometer and Incoherent Scattering (NASA model atmosphere)
NACA	National Advisory Committee on Aeronautics
NORSE	BMD nuclear code (DNA)
NTF	National Test Facility
PEM	nuclear code (DNA)
PT	perturbed density
SDIO	Strategic Defense Initiative Organization
SPIET	BMD engagement code (USA SSDC)
SS-L2	System Simulator-Level 2 (BMD Simulation Code-NTF)
SSGM	Strategic Scene Generator Module (NRL)
STB	Surveillance Test Bed
T_{ave}	average temperature
T_{exo}	exospheric temperature
T_{max}	maximum temperature
T_{min}	minimum temperature
TREM	BMD nuclear engagement code
US-62	model atmosphere representing high geomagnetic activity
US-72	model atmosphere represesenting low geomagnetic activity
USSA	U.S. Standard Atmosphere
USA SSDC	U.S. Army Strategic and Space Defense Command

EXECUTIVE SUMMARY

This document reviews the use of model atmospheres for Ballistic Missile Defense (BMD) engagement modeling. Model atmospheres are standardized representations of atmospheric density and temperature as a function of altitude. Engagement models simulate the flight of a ballistic missile from launch to interception by the BMD interceptor missiles. The simulated engagement takes place in the earth's (upper) atmosphere, and it is modeled using a model atmosphere. The document discusses the application of model atmospheres in ballistic missile targeting, PenAid stripout and discrimination, guidance for direct-impact kill vehicles, "nuclear heave," the lifetime of low-altitude satellites, and the loss rate of kinetic debris.

At present about 30 different model atmospheres are available, and they vary significantly in assumed solar activity, time of day, latitude, and season. The two most frequently used model atmospheres are the US-62 and US-76 models. US-62 represents a period of high solar activity and US-76 represents a period of low solar activity. Figure S-1 compares the two models with respect to atmospheric density and temperature. Density is the most significant parameter for most BMD applications, and, as Figure S-1 indicates, density falls off very rapidly with altitude. Table S-1 shows the apogee (maximum altitude) of ballistic missiles of different ranges. The table indicates the need for model atmospheres up to quite high altitudes.

BMD analysis often employs different model atmospheres in the same engagement. To compare different tactical or system applications it is necessary to use a single model atmosphere as far as possible; this will minimize confusion in the comparison of different tactical or system applications. To determine how large the effects of atmospheric variability are on a particular application, we recommend running the simulation using the US-62 and then repeating the run with the US-76 model. The difference between these two models is about as large a variability as one finds between any two model atmospheres. If there is a difference in the output for the two models, this indicates the need for closer examination of the physics of the particular problem.

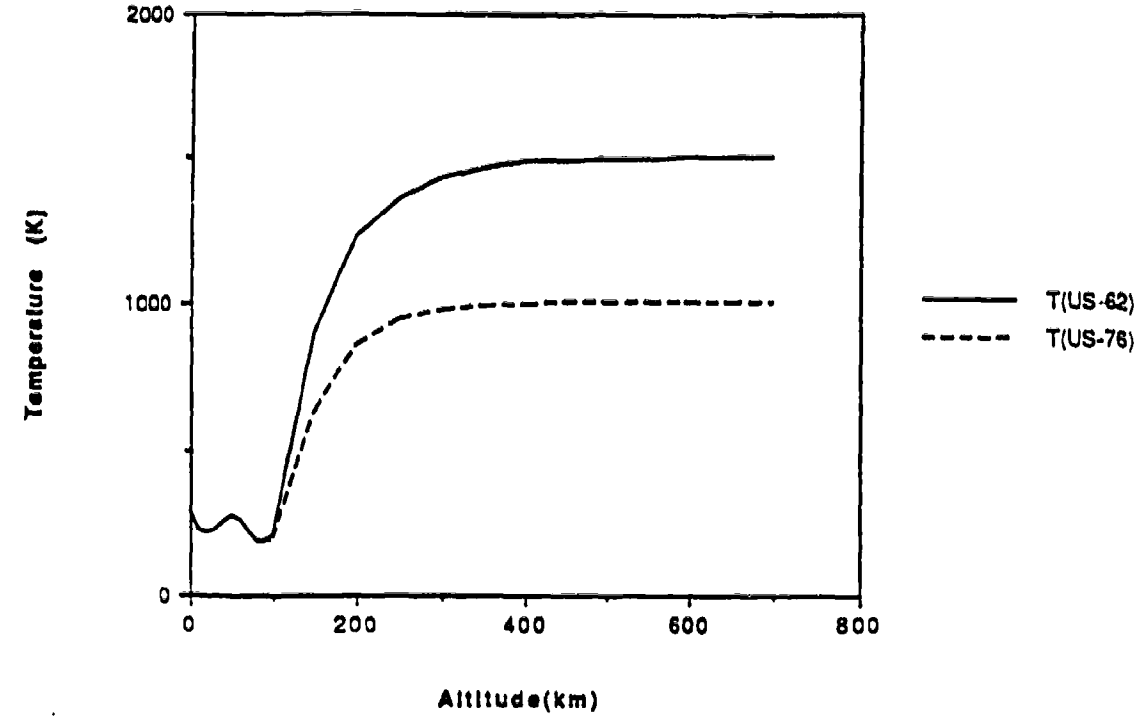

a. Temperature

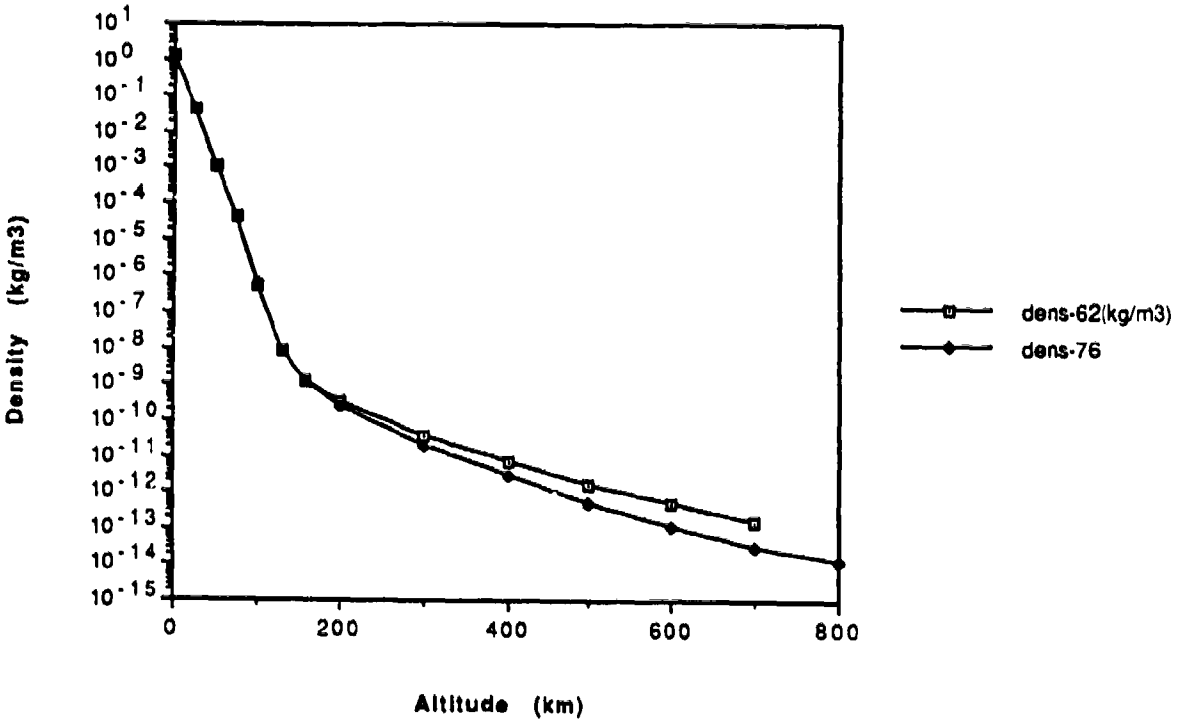

b. Density

Figure S-1. Atmospheric Temperature and Density from US-62 and US-76 Models

Table S-1. Apogee as Function of Missile Range

Range (km)	Apogee (km)	Type of Missile
312.0	88.0	1 stage
600.0	156.0	1 stage
900.0	240.0	1 stage
1500.0	350.0	2 stage
3000.0	660.0	2 stage
10,000.0	1580.0	4 stage

Note that, in addition to the static atmosphere, which varies with latitude, season, time of day, and solar activity, there are other factors such as wind, effects of the non-spherical earth, and a variety of short-term phenomena that may be critical for specific BMD applications.

1. INTRODUCTION: THE UPPER ATMOSPHERE

Ballistic missile defense operations--detection, discrimination, and interception--take place within the atmosphere at rather high altitudes; interception takes place at long ranges (up to several hundred km) at altitudes above 20-30 km.[1] Analyses normally require one to use a model of the atmosphere that gives the atmospheric density and temperature as a function of altitude, with emphasis on altitudes above 100 km where the density is low and the principal variation is solar activity rather than latitude and season.[2]

At present there are at least 30 different model atmospheres in use.[3] Each model atmosphere depicts the atmospheric density and temperature at some specific time and place (for example, at some time in the 11-year solar cycle and in different seasons, latitudes, and times of day). The choice of model atmosphere can affect a broad range of BMD operations. The effects of atmospheric model can be small or large, resulting in dramatic changes in system performance. It is important to identify these cases because when the models give different answers, a closer look at the physics of the problem is needed.

The availability of so many model atmospheres can make intercomparison between simulation analyses difficult and can obscure instances where real atmospheric effects are critical. For instance, for ICBM targeting the difference between summer and winter atmospheres on a given path can amount to a 40-km difference in range, which is obviously critical. Comparable effects arise due to varying winds, day/night density variation, short-time dynamic perturbations,[4] and the effects of a nonspherical earth.

---

1 The (relatively) short-range Patriot missile works at somewhat lower altitudes. *Jane's Land-Based Air Defense Systems*, 5th edition, 1992-93, p. 289, lists a maximum range of 160 km and a maximum altitude of 24 km.

2 A standard or model atmosphere is defined conventionally as a set of temperatures and densities as a function of altitude, with emphasis on altitudes above 100 km where the density is very low (10^{-6} times the sea level value) and the principal variation is solar activity rather than latitude and season. The exospheric temperature (i.e., above 500-1000 km) is relatively large (~1500 K) for high solar activity, and small (~800 K) for low solar activity. Solar geomagnetic activity is parameterized by the Zurich sunspot number R_Z, or the solar flux at 10.7 μm, $F_{10.7}$, and the activity index A_p.

3 See ANSI/AIAA, 1990. Appendix E lists a Standard Atmosphere from the Former Soviet Union, which looks very similar to the US-62 Model Atmosphere. This atmosphere is not included in the ANSI/AIAA compilation.

4 There is a variety of effects on shorter scales due to such processes as tides, acoustic gravity waves, turbulence, etc. See Table 5 and Appendix A-2.

It must be stressed that there is a distinction between a "standard (or model) atmosphere," which is useful for the inter-comparison between different elements of phenomenology and an "actual atmosphere," which describes conditions at a specific space-time location and would serve for targeting or some other high-precision application.

In the System Simulator, which may be used to model a particular type of tactical procedure as part of an overall engagement, the details of a particular model atmosphere are less important than consistency in the atmosphere chosen: a representative standard atmosphere is required, so that when the results of two procedures are compared we know that the difference in result is due to the tactical procedures rather than to the choice of atmospheric models.

In this Section we give a brief overview of atmospheric conditions, while applications to various problems are discussed in Section 2.

Atmospheric density falls rapidly with increasing height, but the effects of even very low densities can be significant for such problems as discrimination between warheads and decoys and the targeting of anti-ballistic missiles. Figure 1 shows the high-altitude temperature and density profiles for the US-62 and US-76 model atmospheres; they differ significantly at high altitudes because the active sun produces enhanced heating of the earth's upper atmosphere, which leads both to a higher temperature and a higher density.[5]

1.1 MODEL ATMOSPHERES IN HISTORICAL PERSPECTIVE

Table 1 sketches the development of model atmospheres in historical perspective.

- The first serious concern with the atmosphere above the tropopause (ca. 11 km) arose in the context of ionospheric radio propagation, when it was realized that long-range radio wave propagation involves reflection of radio waves from the ionosphere at 100- to 200-km altitude.
- There was some concern with aiming long-range artillery as early as World War I. The V2 rocket in World War II had an apogee ca. 70 km; however, its accuracy was so low that the effect of upper atmospheric drag was not significant for its military mission. In the 1947-52 time period a number of V2 rockets were flown from White Sands Missile Range to explore the upper atmosphere, and they provided some data up to ~ 200 km.

---

5 The US-62 model (Valley, 1965, p. 2-19 ff.) corresponds to high solar activity, while the US-76 model (U.S. Standard Atmosphere, 1976) corresponds to low solar activity. While the US-62 model atmosphere is widely used, it is now considered an extreme rather than a representative model.

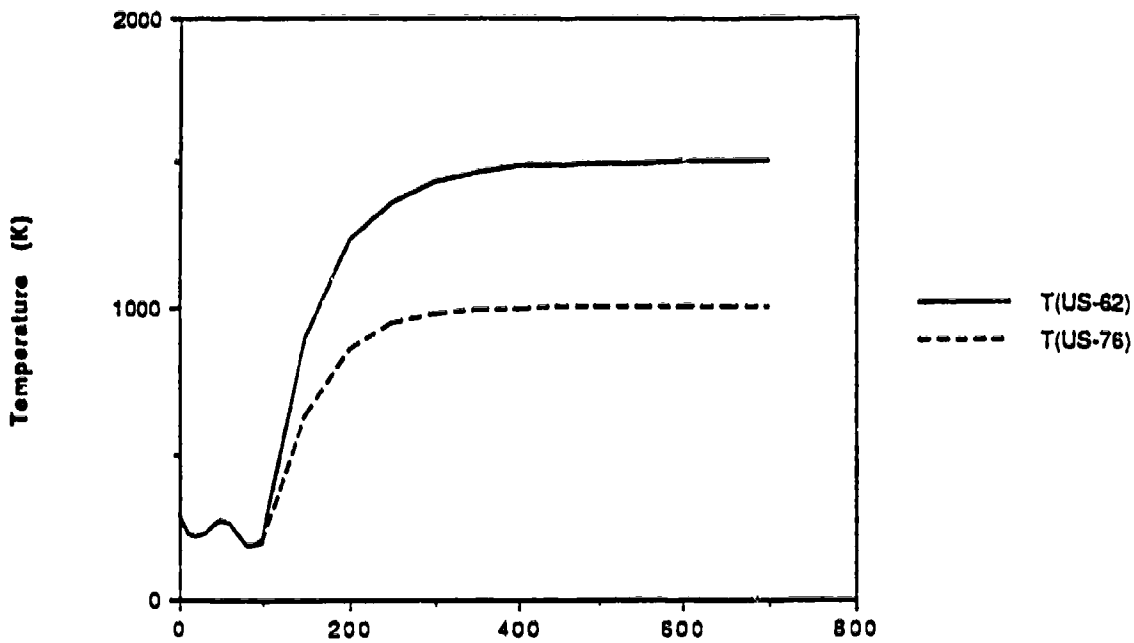

a. Temperature

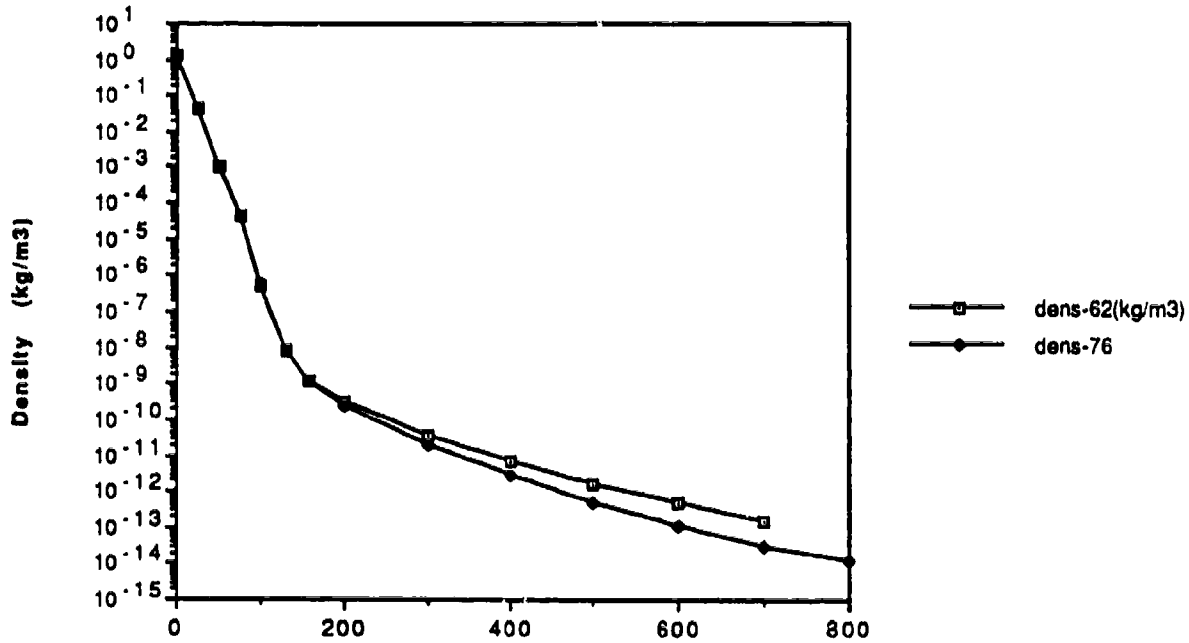

b. Density

Figure 1. Atmospheric Temperature and Density from US-62 and US-76 Models

Table 1. Model Atmospheres in Historical Context

Date	Application of Interest	Model Atmosphere
pre-WW-II	• Aviation unpressurized, to 6 km; pressurized, to 10 km • Long-range artillery; density to 20 km in 1918 • HF radio waves reflected from ionosphere (100-200 km)	Different regions/seasons to 15 km
WW-II	V-2 rocket , apogee 70 km; inaccurate, so high-altitude drag not significant	
1954	• Jet aircraft to 15-20 km	NACA[a] and ICAO[b] models needed to 20 km
1956	• Aircraft, rockets; low-altitude satellites anticipated	ARDC[c]-56 model to 1000 km
1958	IGY[d]: Coordinated international research program; satellites (Vanguard, Sputnik, etc., planned for this). This happened to coincide with the largest solar maximum yet observed, R_Z to 280 (normal maximum ~ 100).	
1959	IGY shows that high-altitude density of ARDC-56 is too high by factor 20	ARDC-59 corrects
1961	First International Standard Atmosphere to high altitudes	CIRA[e]-61
1962	New U.S. model atmosphere--uses data from IGY, i.e., high solar activity	US[f]-62
1965	Revision of CIRA-61	CIRA-65
1966	Supplements (variations with latitude and season) to USSA-62	1966 Supplements
1971	Solar minimum (R_Z as low as 0-10)	
1972	Revised CIRA model	CIRA-72
1976	New U.S. Model Atmosphere, corresponds to low solar activity	US-76
1980s	NASA MSIS[g]	MSIS-83, 86
1988	Revised CIRA model	CIRA-86
1990	Revised MSIS model, Hedin, 1991	MSIS-90

[a] National Advisory Committee on Aeronautics (predecessor agency to NASA).
[b] International Civil Aviation Organization (U.N. agency).
[c] Air Research and Development Command (USAF agency).
[d] International Geophysical Year.
[e] COSPAR (Committee on Space and Atmospheric Research) International Reference Atmosphere.
[f] U.S. Standard Atmosphere.
[g] Mass Spectrometer and Incoherent Scattering (models based on high-altitude in situ and remote sensing measurements).

NOTE:
- USSA models give a diurnal average, while CIRA models specify local time and geomagnetic activity.
- Many people have used US-76 for low geomagnetic activity, CIRA-65 Model 5/h8 for average geomagnetic activity, and US-62 for high activity.
- MSIS-90 specifies latitude, season, etc., is available on magnetic tape only.

- With the development of jet aircraft, which fly up to 45,000 ft (15 km), there was concern about atmospheric models up to 20 km. The U.S.A.F. developed the ARDC (Air Research and Development Command) model atmospheres in the context of high-altitude rockets and the International Geophysical Year (IGY). It turned out that the IGY (1957-58) corresponded to the largest solar maximum ever observed, and thus the US-62 model atmosphere is more extreme than had been supposed. In 1966, supplements for seasonal and latitude variations from the US-62 model were introduced. The US-76 standard corresponds to low solar activity.
- In parallel with the U.S. developments, there was also a (largely European) set of standards as the CIRA (COSPAR International Reference Atmosphere) series, with versions in 1961, 1965, 1972, and 1986. This includes variation with solar activity and with time of day, recently also with latitude. Most recently the NASA MSIS (Mass Spectrometer and Incoherent Scatter) models have provided a great deal of information, including variation with latitude, longitude, time of day, and solar activity. At present over 30 model or standard atmospheres exist for different conditions (see ANSI/AIAA, 1990).

Atmospheric conditions are also variable at low as well as high altitudes, and on a variety of time scales: Appendix A presents some results. Appendix A-1 shows results on long-term variability, principally from the U.S. 1966 Supplements (to the US-62 model atmosphere) and from the US-76 model. Thus, e.g., at 50 km, the 1 percent extreme limits of temperature are 200 and 310 K, while the density varies from – 60 percent of its mean value at a given altitude to + 40 percent.[6] Appendix A-2 shows results for a variety of shorter period dynamic processes, on periods from diurnal and semi-diurnal tides down to various kinds of waves having periods as low as a few minutes.

1.2 DEFINITION OF VARIOUS MODEL ATMOSPHERES

Because the atmosphere is so variable, a large number of different "standard" or "model" atmospheres have been developed. A Standard Atmosphere is defined conventionally as a set of densities and temperatures as a function of altitude with emphasis on altitudes above 100 km. The principal variation is with solar activity (both electromagnetic radiation--i.e., time of day--and charged particle emission) rather than with latitude or season. Solar magnetic activity (the 11-year cycle) is normally expressed by $F_{10.7}$, the microwave flux at 10.7 cm wavelength as recorded in Ottawa rather than by the Zurich sunspot number. A measure of charged particle activity is given by the index A_p.

---

6 There is also a variation with latitude.

The exospheric temperature T_{exo} varies from about 1000 K at low solar activity to 1500 K at high activity; there is a corresponding variation in density.

A current compilation (ANSI/AIAA, 1990) presents some 30 distinct models that go to high altitudes. Table 2 shows the model atmospheres that are actually used in a variety of engagement-level and phenomenology codes employed in BMD and other modeling. US-62 (representing high geomagnetic activity) is used in some codes, US-76 (representing low geomagnetic activity) is used in other codes, while CIRA-65 Model 5/h8 (representing average geomagnetic activity) is used in still other codes.

Table 2. Atmospheric Models Used in Different Codes

Type of Code	Name	Atmosphere Used[a]	Source
Engagement			
	AMEM	US-62 (and S-66)[b] and CIRA-65, Model 5/h8 (above 120 km)	Fisher and Byrn, 1991
	SPIET	US-62 (and S-66) and CIRA-65, Model 5/h8 (above 120 km)	Christie Harper, SPARTA, Huntsville, AL
	SS-L2	(a) US-62 and US-76 as default, and TREM for nuclear environments[c]	Fisher and Byrn, 1991
	STB	"Very flexible - Compatible with SSGM"	Bradley Biehn, Martin-Marietta
Threat Tape		US-62[d]	G. Simonson, NTF
SSGM		US-76 as default	Fisher and Byrn, 1991
Nuclear	NORSE	(a) US-62 (and S-66) and CIRA-65, Model 5/h8 (above 120 km)	Fisher and Byrn, 1991
		(b) Above 120 km, model 10.7 cm flux and season	John DeVore, Visidyne
	SCENARIO	CIRA-65, Model 5/h8 (Code only works above 120 km)	Bill White, MRC
	TREM	US-62 (and S-66) and CIRA-65, Model 5/h8 (above 120 km)	Fisher and Byrn, 1991
	HiSEMM	Analytic fit to CIRA-65, Model 5/h8	Jay Jordano, Visidyne
	PEM	Fit to NORSE - no user choice	Tim Stephens, Visidyne
Kinetic Debris	DEBRA	None	
	KIDD		

[a] Frequently default only. The US-62 model corresponds to *high* solar activity, CIRA-65 Model 5/h8 corresponds to *average* solar activity, and US-76 to *low* solar activity. See, e.g., Table 3a.

[b] S-66 refers to the 1966 Standard Atmosphere Supplements to the 1962 Standard Atmosphere.

[c] There may be some inconsistency here.

[d] Non-zero density only below 300 kft.

At high altitudes the most dramatic variation is the exoatmospheric (high-altitude) temperature, as one can see from Fig. 1. This in turn depends on solar activity which varies with the 11-year sunspot cycle. Table 3 gives the correlation of several commonly used model atmospheres with solar activity. We show the exospheric temperature and the solar activity as parameterized by the 10.7-cm solar flux, $F_{10.7}$,[7] and also the geomagnetic activity index A_p.[8] Note that the US-62 and US-76 models give diurnal averages, while the CIRA-65 model also shows variation with local time of day.

Table 3. Representation of Solar Activity in Different Model Atmospheres

a. Various Models

Solar Activity	$F_{10.7}$ (10.7 cm solar flux)	A_p (measure of particle activity)	T_{exo} (exospheric temperature)	Model Atmosphere
L, Low	75	2	~ 800	US-76
	70	4	730	CIRA-86
M, Medium	150	6	~ 1200	CIRA-65, Model 5/h8
	150	4	1037	CIRA-86
H, High	250	12	~ 1600	US-62
	230	4	1253	CIRA-86

b. Temperature vs. Altitude as Function of Solar Activity (from CIRA-86 Model)

	Altitude (km)		
	100	400	1500
Solar Activity	Temperature (K)		
L, Low	187	736	736
M, Medium	185	1037	1037
H, High	183	1251	1253

---

7 $F_{10.7}$ is the slowly varying component of the solar power flux density at 10.7 cm wavelength which has been measured regularly at the National Research Council, Ottawa, Canada, since 1947. It correlates rather well with the Zurich sunspot number--see, e.g., Valley, 1965, p. 16-21 ff.

8 There are a number of different geomagnetic activity indices, which are defined in Jursa, 1985, p. 4-27 ff.

The variation of atmospheric temperature with time of day is of magnitude comparable to that due to solar activity. Table 4 (taken from CIRA-65) shows this in a lot of detail. Explicitly, the difference in high-altitude temperatures of US-62 and US-76 is 500 K, while for CIRA-65, the difference between 1400 and 400 local time for models 2 (low activity), 5 (average activity), and 9 (high activity) is 320 K, 450 K, and 600 K, respectively.

Table 4. CIRA-65 Model Temperature (K) Variability with Solar Activity and Local Time[a]

CIRA 65 Model	$F_{10.7}$ (10.7 cm solar flux)	A_p (measure of charged particle activity)	T_{max} (1400 LT) (K)	T_{min} (0400 LT) (K)	ΔT (K)
2 (Low Solar Activity)	75	2	1064	731	333
5 (Medium Activity)	150	6	1460	979	481
9 (High Activity)	250	12	1969	1317	652

[a] For comparison, US-76 gives T_{ave} = 1000 K while US-62 gives T_{ave} = 1500 K.

T_{max} = maximum temperature; T_{min} = minimum temperature; T_{ave} = average temperature.

Note, however, that the principal operative parameter for system operability is atmospheric density rather than temperature. Here the diurnal variations are significantly smaller than those with solar activity. Thus Fig. 2 gives density variations as a function of altitude with day/night and solar activity (measured by the $F_{10.7}$ parameter); for example, at 200 km the diurnal density variability is only about 20 percent while the solar cycle variability is about 80 percent.

There is also a significant variation in density (and in temperature) with latitude. Figure 3 compares density profiles for day/night and solar activity variations for latitudes 0° and 80°; note that at 500 km the variation is more than a factor of 10!

Finally, there is a natural variability in densities due to dynamic processes on various short-time effects such as acoustic waves, turbulence, etc.[9] Table 5 indicates the characteristics of short-term upper atmospheric density variations which represent

---

[9] In fact, aircraft flying at high altitudes (above ~ 15 km) may experience flight instabilities due to short-term changes in atmospheric density.

fluctuations about the mean values specified in the model atmospheres. Appendix A-2 shows some "representative" examples and explains some of the terms used here. Note that this does not specify how frequently these effects occur, simply that fluctuations up to 10-50 percent about the mean density must be expected.

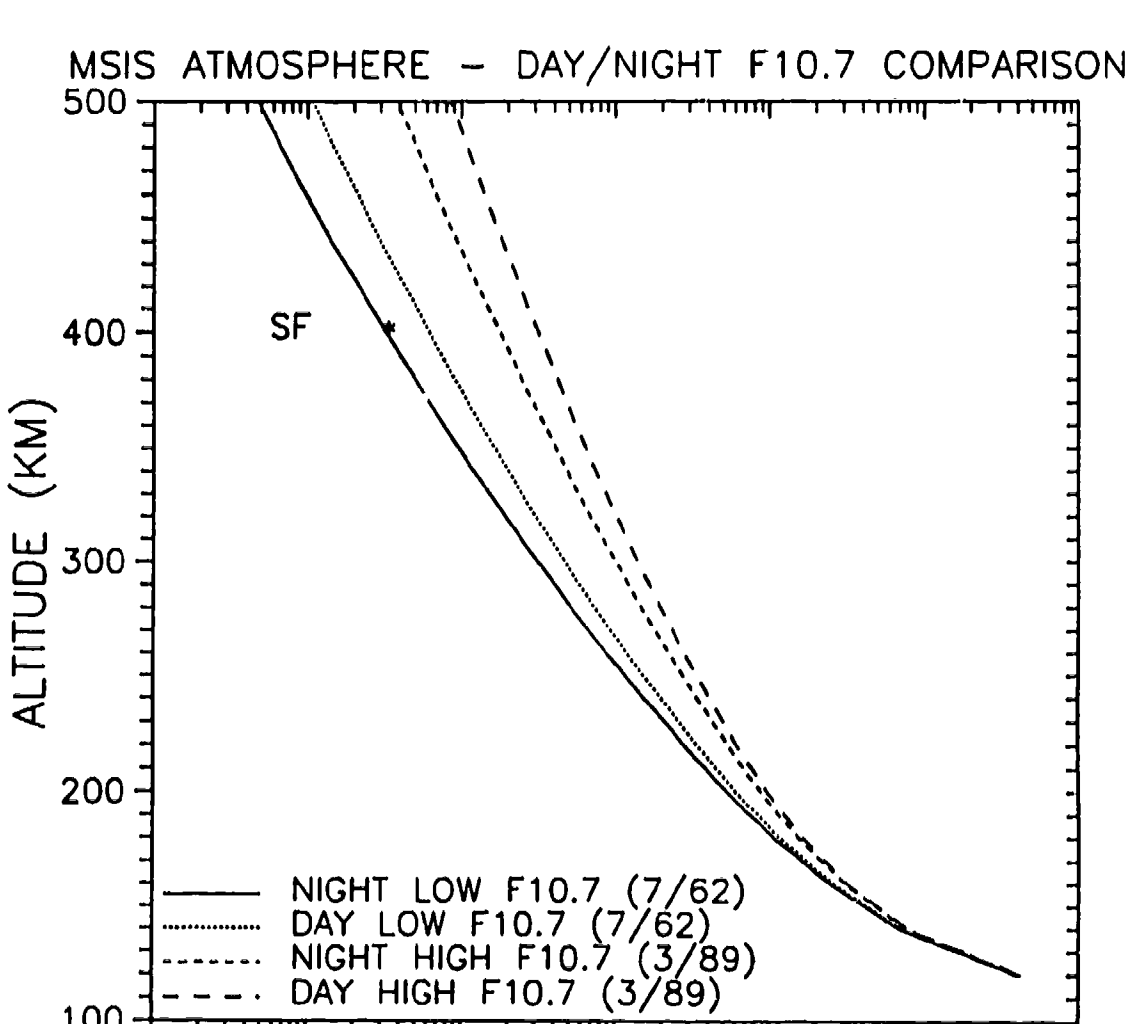

Figure 2. (Latitude-Averaged) Density as a Function of Altitude for Day/Night Conditions at Low and High Solar Activity (as measured by the $F_{10.7}$ Index). Data provided by R. Armstrong, MRC, using the NASA MSIS-90 model atmosphere (Hedin, 1991).

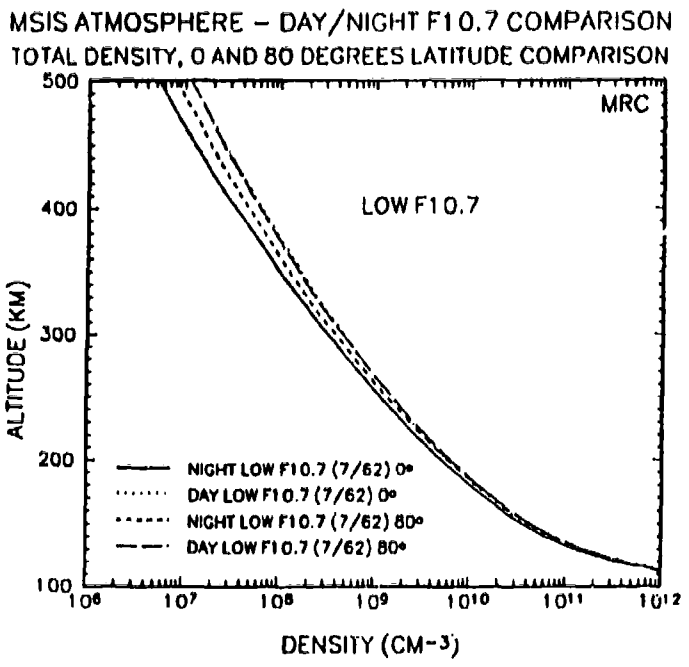

A. Low Solar Activity (as measured by the $F_{10.7}$ Index)

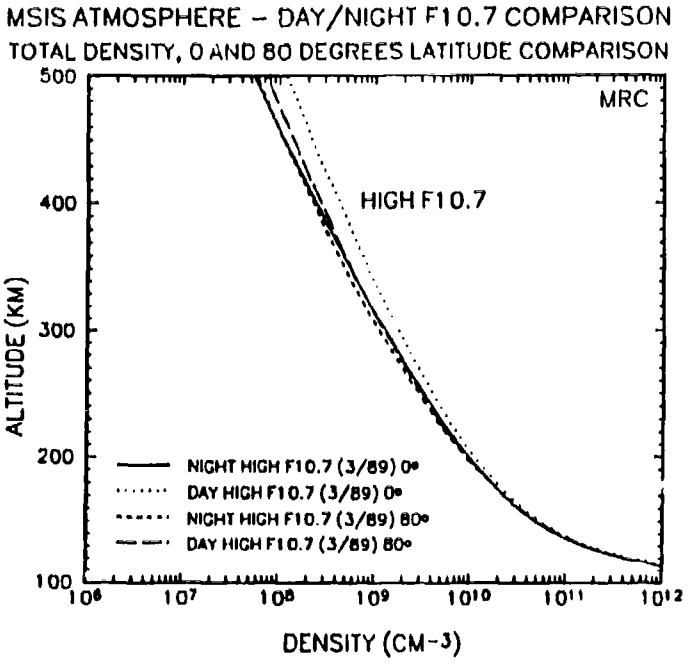

B. High Solar Activity

Figure 3. Density as a Function of Altitude for Day/Night Conditions at 0° and 80° Latitude. Data provided by R. Armstrong, MRC, using the NASA MSIS-90 model atmosphere (Hedin, 1991).

Table 5. Short-Term Upper Atmospheric Density Variations (Source: Humphrey et al., 1981--see Appendix A-1 for more explanation)

Time Scale (period)	Amplitude, $\Delta\rho/\rho_{av}$ (%)	Altitude variation (km)
Deterministic		
Semidiurnal (12-hr) tide	20-50	increases to ca. 180[a]
Random		
Acoustic-Gravity waves (AGWs)[b]		
5-15 min	10-30	increases to ca .100
Turbulence[c]		
1-5 min	10-30	increases to ca. 110-120

a Diurnal (24-hr) tides become more important above this altitude.

b Atmospheric disturbances at low altitudes due to thunderstorms, etc., amplify in traveling up (ρu^2 ~ constant, where u = velocity) until they "break" near 100 km. When the waves break, their energy is transformed into turbulence, typically on somewhat shorter periods. The name AGW comes from the fact that the restoring force of the waves is provided by gravity rather than by compressibility, as for higher frequency sound waves--see Appendix A-2 and the definition of the Brunt-Vaisala frequency N.

c Random disturbances (of higher frequencies/shorter wavelengths than AGWs) which amplify up to the turbopause, above which the atmospheric density is so low that the atmosphere can no longer sustain these motions.

Reference to the ANSI/AIAA 1990 compilation shows that some model atmospheres have much more detail than others. Thus the NASA MSIS-90 atmosphere presents mean values as a function of latitude, longitude, and season as well as time of day and solar activity. While this level of detail (and more) is needed for some applications--such as missile targeting--it is not appropriate for the engagement modeling provided by the various BMD test beds that are used for simulating different aspects of the BMD system.[10]

From the present discussion we note that the US-62 and US-76 model atmospheres are not to be regarded as either "good" or "upper and lower bounds," yet they are both widely used and not implausible. Furthe., the difference between these two models is typical of the difference between atmospheric conditions at different latitude, season, time of day, and solar activity. Thus a low-cost empirical way of establishing the effect of

---

10 There may be a difference in requirements between Research and Development Test Beds like the System Simulator and the Surveillance Test Bed, and an Operational Test and Evaluation Test Bed such as ISTC (Integrated System Test Capability).

atmospheric variability on a designated phenomenon is to run the appropriate engagement model using both US-62 and US-76 atmospheres. If the results are essentially the same, then the choice of model atmosphere is probably not critical; if the results differ to a significant extent, this is an indication that a closer investigation of the problem is required.

2. APPLICATIONS AND ISSUES

2.1 OVERVIEW

For orientation, I have itemized various applications in which atmospheric models are currently used, to indicate what kind of uncertainties and variabilities can be expected. These examples show that even the effects of the very low atmospheric density at high altitudes (> 100 km) can be important for a variety of BMD applications, such as discrimination, and thus the choice of the atmospheric model is significant. Table 1 (above) indicates that different phenomenology and engagement models used for BMD application use different model atmospheres. Since there now exist some 30-odd distinct atmospheric models, the problem of standardization can be severe.

First, Section 2.2 notes that any simulation is subject to different kinds of uncertainties, and one should not ask questions of the simulations whose answers cannot be well defined. Section 2.3 points out that low-altitude density and wind, and the non-spherical shape of the earth all have significant impact on ballistic missile trajectories. Section 2.4 discusses the peak deceleration and the "stripout" of penetration aids which occur at different altitudes from 85 to 150 km for reentry vehicles and various types of decoys. Section 2.5 says that the very precise targeting needed for direct impact kinetic kill vehicles gives very severe constraints on how accurately one must know atmospheric drag and, thus, density as a function of altitude. Section 2.6 discusses "nuclear heave," the nuclear-induced buoyant lifting up of large atmospheric air parcels above 150-200 km. Section 2.7 points out that the lifetimes of low-altitude orbiting satellites vary significantly with solar activity. Section 2.8 presents the loss rate of kinetic debris as varying greatly with solar activity as well as altitude.

2.2 TWO KINDS OF UNCERTAINTIES

In any engagement modeling (or other kind of simulation) there are two different types of uncertainties: one type can be reduced or resolved by more measurement and analysis; the other type cannot be reduced because it depends on factors that are inherently unresolvable at the level of a simulation [such as the short-term variations of Table 5 (above) or Appendix A-2].

A simulation should be designed with the recognition of these two kinds of uncertainties, so that the user will not ask for details that are inherently not determinable and will have reasonable expectations of what a computer simulation can and cannot do.

2.3 BALLISTIC MISSILE TRAJECTORIES: EFFECTS OF DENSITY, WIND, AND SHAPE OF THE EARTH

Winds and densities--in particular in the lower atmosphere--affect ballistic missile accuracy significantly. Appendix B is the abstract of an IDA paper written by R.G. Finke in 1969 which discusses the effects of winds and of density variation in the lower atmosphere on ballistic missile accuracy. Finke concludes that for a high-performance ICBM the most important effects come from low-altitude variations in wind and density. His calculations show that for 5-km layers centered at 5 and 10 km, a 1-percent change in density or 0.3-m/sec change in wind speed leads to perhaps a 200-m target error. This is a basic analysis that ought to underlie any of the more sophisticated treatments that can be employed nowadays. (In fact, newer and more sophisticated calculations of density effects frequently do not include the effects of winds.)

Figure 4 gives a frequency distribution of (scalar) winds with altitude at a specific location. It is presented here to point out that the effects of wind and of its variability must be considered, to be sure that they are not significant for a particular application. As one example, the difference between the 50th and the 75th percentile of wind speed at 6 km is 9 m/sec. In Table 6 we show the ballistic missile range error due to a 9-m/sec wind and a 15-percent change in density, both in the 5-10 km altitude range, for various values of missile ballistic coefficient $\beta = W/C_D A$, for both ICBM and IRBM conditions. We see that for reasonable vehicles ($\beta \sim 1000$ lb/ft^2 or 4900 kg/m^2) range errors on the order of fifty to several hundred meters are possible. The range error is proportional to the wind speed as well as to the transit time through the region in which the wind is blowing. Table 6 shows that the effect of wind speed can be significant for some applications.

Ballistic missile targeting is affected both by details of the atmosphere and by the precise shape of the earth that is assumed. P. Kysar, IDA (unpublished work), used the IDA RANGE code to determine the effects of the atmosphere on the range of a given ICBM, and finds the results shown in Table 7 for the effects of the different model atmospheres for a "representative" ICBM: the effective range of an ICBM varies by some 20-40 km with season, purely as a consequence of the different atmosphere. The large ICBM used in this analysis travels farther in summer and winter than in spring or fall.

Altitude (km)	Percentile				
	50	75	90	95	99
1	7	10	13	15	19
6	20	29	36	41	50
10	31	43	53	60	73
11	32	44	55	62	79
12	32	44	55	62	79
20	6	10	14	17	26
23	6	10	14	17	26
40	55	67	82	90	105
50	79	96	111	120	132
58	83	107	128	140	164
60	83	107	128	140	164
75	50	65	87	98	118
80	50	65	87	98	118

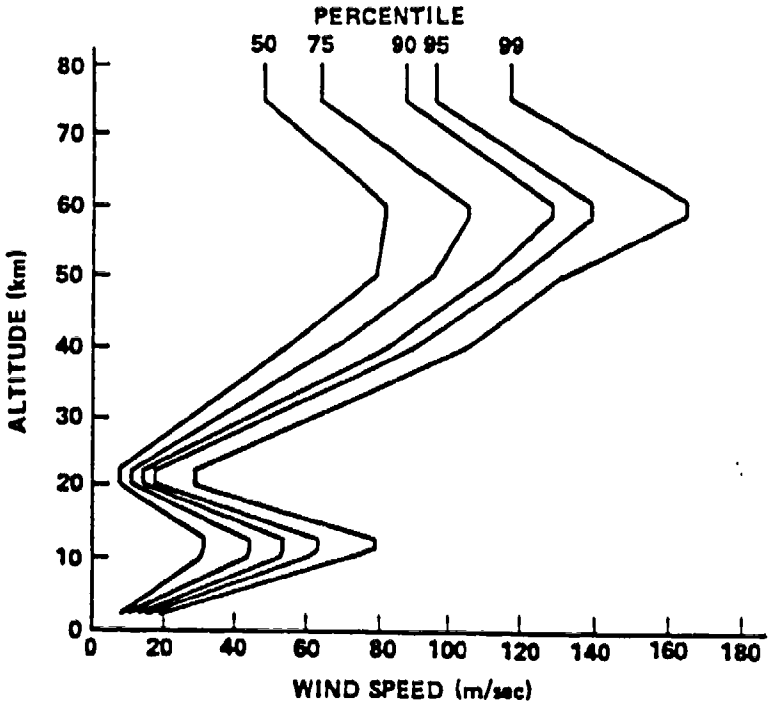

Figure 4. Scalar Wind Speed Distribution at Vandenberg AFB, CA (Source: Turner and Hill, 1982)

Table 6. Ballistic Missile Miss Distance Contribution Due to a 5-km Layer Between 5 and 10 km Altitude of Winds (9 m/sec) and 15-Percent Changes in Density, for Different Ballistic Coefficients and ICBM and IRBM Conditions (Source: Finke, 1969)

ICBM: velocity v_0 = 22,500 ft/sec (6.86 km/sec), reentry angle γ = 25°			
Ballistic coefficient β (lb/ft^2)[a]	550	1025	1975
Miss distance (m) due to 9 m/sec wind	160	54	12
Miss distance (m) due to 15% density change	480	190	22
IRBM: velocity v_0 = 15,000 ft/sec (4.57 km/sec), reentry angle γ = 30°			
Ballistic coefficient β (lb/ft^2)[a]	550	1025	1975
Miss distance (m) due to 9 m/sec wind	1400	360	130
Miss distance (m) due to 15% density change	500	110	14

[a] 1 lb/ft^2 = 4.9 kg/m^2

Table 7. Effect of Changes in Model Atmosphere on ICBM Trajectories (US-62 Atmosphere and US-1966 Supplements) (Source: Kysar, IDA, private communication)

	Spring and Fall[a]	Winter	Summer
Range (km)	9948.3	9978.2	9968.6
Apogee (km)	1315.2	1291.6	1298.9
Travel time (sec)	2103.1	2135.7	2138.3

[a] US-62 Average for spring and fall, variations for winter and summer values.

The nonspherical shape of the earth (flattening) leads to effects on ballistic missile targeting of the same order as the atmospheric effects considered here, some 20-40 km at ICBM ranges, and thus they should be included as appropriate.[10] Appendix C gives a brief overview of some numerical descriptions of the earth's shape.

2.4 DISCRIMINATION AND PENAID STRIPOUT

If discrimination is possible at deceleration in the range 0.1 g or 0.01 g, then the relevant discrimination altitudes for a balloon (β = 1 lb/ft^2), for a decoy (β = 30 lb/ft^2), and for an RV (β = 1000 lb/ft^2) are listed in Table 8. These results come from current calculations of R.G. Finke, IDA, using the IDA RANGE Code (which uses the US-62

[10] There are comparable effects on shorter range ballistic missiles and on the targeting of kinetic kill vehicles aimed at ballistic missiles.

Model Atmosphere). Figure 5 (from R. Finke, IDA, work in progress) shows representative values for deceleration vs. altitude for balloons, replicas, and RVs computed with the IDA RANGE code.[11] If a radar can detect a deceleration of 0.01 g, this suggests that a balloon can be identified at ~145 km, whereas a 1/10 scale decoy cannot be positively discriminated above ~ 95 km.

Table 8. Discrimination Altitudes for RVs and PenAids for Different Values of Deceleration (Source: R.G. Finke, IDA)

	Altitude (km)		
Deceleration	Balloon	Decoy	RV
0.01 g	145	110	80
0.1 g	120	88	75

If the density varies by a factor of – 25 percent to + 50 percent (cf., e.g., Fig. A.2 in Appendix A) then the altitude for discriminating a balloon varies from perhaps 140 to 160 km, while that for discriminating an RV ranges between 80 km and 95 km.

Note that because of the range of variation as represented by the US-1966 Standard Atmosphere Supplements, it is necessary to consider the effects of non-zero atmospheric densities up to at least 150-180 km. [Some trajectory models in current use employ a spherical earth with non-zero density only below 300 kft (92 km).]

2.5 ABM TARGETING FOR KINETIC KILL

The use of direct impact kinetic kill by interceptors--with acceptable miss distances less than 1-3 m--may give rise to severe constraints on how accurately one must know atmospheric drag. A quantitative analysis of this problem depends on the details of the interceptor vehicle and its control mechanisms as well as on the effective drag term employed. As in Section 2.3, the effects of atmospheric density and wind and possibly the nonspherical shape of the earth will be important here.[12]

In fact, here is a case where use of a single density model may give unreliable results.

---

11 G. Naidenko, 1991a, has discussed this problem also.

12 I am not aware of any such calculation having been performed.

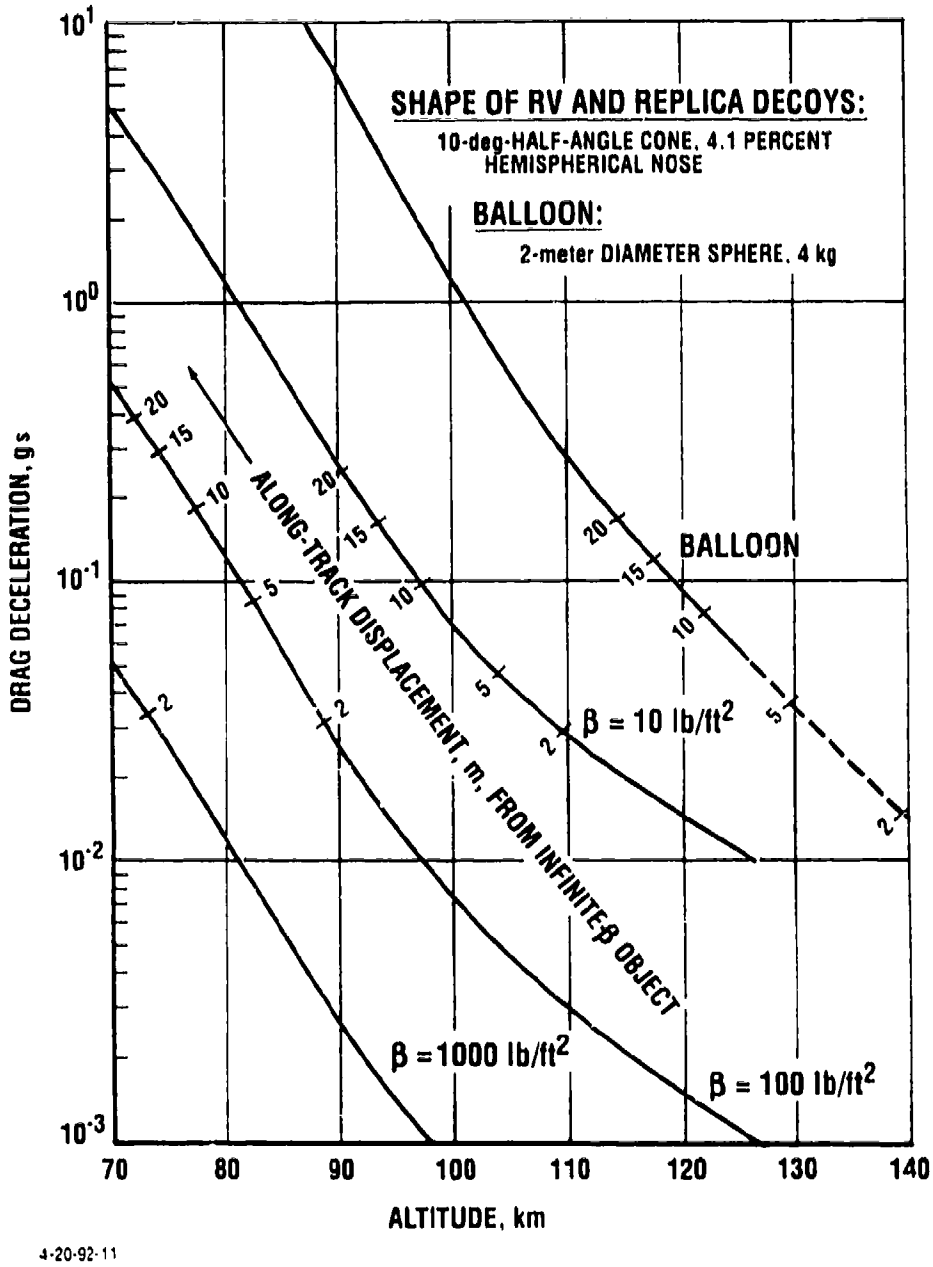

Figure 5. Calculated Drag Deceleration at High Altitudes for Different Objects (Reentry Velocity 7 km/sec; Reentry Angle = 25° at 150-km Altitude; US-62 Model Atmosphere) (Source: Finke, IDA)

2.6 NUCLEAR-PERTURBED ENVIRONMENT

In the case of multiple nuclear explosions, such as occur in a ladder-down or a salvage-fuzed scenario for a "Phase I" threat scenario, the atmospheric density can be changed so drastically that the use of a normal model atmosphere is inadequate. In particular, at altitudes above 150-200 km where the air density is greatly enhanced from a very low ambient value by air "heaved up" from lower altitudes, one has to use nuclear environment codes such as NORSE or SCENARIO. Figure 6 shows how the density above 200-500 km can be enhanced by several orders of magnitude as a result of a massive nuclear engagement.[13]

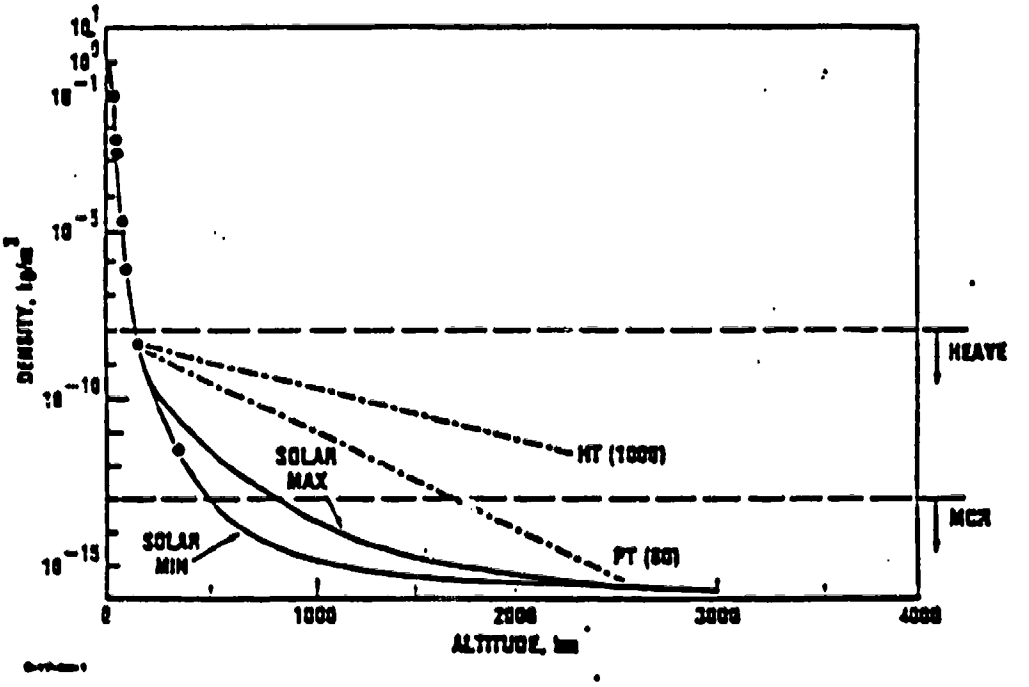

Figure 6. Normal and Heaved Atmospheric Density as Function of Altitude. We show the ambient density corresponding to low and high solar activity, and the perturbed density PT(60) along the plume corresponding to 60 1-Mt bursts, and the general heave HT(1000) corresponding to 1000 1-Mt bursts (from SCENARIO Simulation MS 1.1) (Source: Bauer, 1990)

---

13 With the current (1992) "GPALS" threat, which is very much lighter than the previous "Phase I" threat, the nuclear perturbation is of course much less than that shown in Fig. 6, and thus this effect will hardly ever be expected to occur.

Naidenko, 1991b, has addressed the detection and discrimination of a balloon[14] by a ground-based radar in a nuclear-perturbed environment. The drag force on a vehicle of mass M is given by the expression

$$M\,a = C_D\,A\,\rho\,V^2 \qquad (1)$$

where

C_D = drag coefficient (dimensionless, taken equal to 2)

A = projected area

ρ = effective density of ambient air

V = effective velocity of vehicle.

Naidenko presents calculations with the NORSE code for a 1 Mt explosion at 120 km altitude, 2 min after the detonation. The heave velocity which contributes to V (which enters as V^2) can be 15 km/sec or greater, significantly larger than the ICBM reentry velocity of 7 km/sec. The density is also enhanced (perhaps by a factor of two) by the air that is heaved up. Table 9 shows a significant difference in deceleration of a balloon between the ambient and the nuclear-disturbed atmosphere, even at very high altitudes.[15]

2.7 LOW-ALTITUDE SATELLITE LIFETIMES

For a low-altitude orbiting satellite, the lifetime depends significantly on the level of solar activity. Appendix D demonstrates that for a very low altitude (400-km) satellite a variation in lifetime by a factor of 10 or more is possible.

Table 9. Deceleration of a Balloon in the Ambient and Nuclear Disturbed Atmosphere. Schematic--see Section 2.7 (Source: Naidenko, 1991b)

Altitude (km)	Deceleration in ambient atmosphere (g)	Deceleration in nuclear-perturbed atmosphere (g)
500	-	0.012
400	-	0.02
340	2.9×10^{-4}	0.036
300	6.6×10^{-4}	0.06
200	0.01	0.56

[14] Radius 1 m, mass 1 lb, i.e., not identical with the model of Section 2.4 and Fig. 5.

[15] It must be stressed that the heaved air falls back to its original altitude in 5-10 minutes, so that the scenario discussed here--even apart from the possibly somewhat large values of V used in Table 8--will apply only to a small space-time region in a Phase I scenario involving a massive nuclear engagement. It does not apply for the current INMD/GPALS scenarios.

2.8 LOSS RATE OF KINETIC DEBRIS

The physics of the problem is similar to that in Sections 2.3, 2.4, and 2.7 above, but the numbers may be different. The quantitative loss rate will depend critically on the shape and size of the kinetic debris particles.

3. CONCLUSIONS AND RECOMMENDATIONS

Engagement models simulate the flight of a ballistic missile attack from launch to interception. This engagement takes place in the earth's atmosphere and requires the use of a unified description of atmospheric density and temperature as a function of altitude, i.e., a model atmosphere. For BMD simulations it is important to use a single model atmosphere to minimize confusion in the intercomparison of different tactical schemes for system applications.[15] To determine how large the effects of atmospheric variability are on a particular application, the author recommends running the simulation using the US-62 model and then repeating the run with the US-76 model. The difference between these two models is about as large a variability as one finds between any two model atmospheres.[16] If there is a difference in the output for the two models, this indicates the need for closer examination of the physics of the particular problem.

The following points should be noted:

1. The most critical atmospheric parameter is normally density, which falls off drastically with altitude; for targeting and other high-precision applications (see Section 2) a non-zero density may need to be considered up to 150-180 km where the density is on the order of 10^{-9} of its value at sea level.
2. It must be recognized that the atmosphere varies with latitude, season, time of day, and solar activity. Above 100-200 km the variation of density with solar activity is often the largest single effect, so that the difference between US-62 and US-76 models may well be the largest single measure of variability.
3. In addition to these effects, there are other factors--such as wind, the non-spherical shape of the earth, and a variety of short-term phenomena--that may be critical for specific BMD applications.

---

[15] Reference to Table 2 shows that this may not be a trivial requirement.

[16] Reference to Table 4 in Section 2 and to Appendix A-2 indicates that short-term density fluctuations of up to 10-50% from the mean values given by the Standard Atmosphere Models must be expected.

BIBLIOGRAPHY

ANSI/AIAA, *Guide to Reference and Standard Atmosphere Models*, Report G-003-1990, August 1990.

Banks, P.M., and G. Kockarts, *Aeronomy*, Academic Press, NY, 1973.

Bauer, E., *Uncertainties in the Prediction of High-Altitude Nuclear Effects*, IDA Document D-721, May 1990.

Eckart, C., *Hydrodynamics of Oceans and Atmospheres*, Pergamon, 1960, p. 59.

Feodos'yev, V.I., *Basic Technology of Rocket Flight*, Nauka, Moscow, 1981 (in Russian).

Finke, R., *Reentry Vehicle Dispersion Due to Atmospheric Variations*, IDA Paper P-506, August 1969.

Fisher, J.H., and N.R. Byrn, *DEMVAL Reference Atmosphere*, Nichols Research Corp., NRC-TR-91-187, draft, October 1991.

Hedin, A.E., "Neutral Atmosphere Empirical Model from the Surface to the Lower Exosphere - MSIS - 90," *J. Geophys. Research* 96, 1159, 1991.

Hines, C.O., *The Upper Atmosphere in Motion*, American Geophysical Union Monograph, 18, 1974.

Humphrey, C.H., et al., *Atmospheric Infrared Radiance Variability*, AFGL-TR-81-0207, 1981.

Jursa, A.S., *Handbook of Geophysics and the Space Environment*, USAF, AD/A 167 000, 1985.

Koelle, H.H., Ed., *Handbook of Astronautical Engineering*, McGraw-Hill, New York, 1961.

McIlveen, J.F.R., *Basic Meteorology - A Physical Outline*, Van Nostrand-Reinhold, 1986.

Naidenko, G., *High Altitude OPINE Beta-Discrimination Analysis for GBR (U)*, PRI-H-91-022, 4 February 1991a (SECRET).

Naidenko, G., *OPINE Beta-Discrimination Effects of Heave (U)*, PRI-I-91-113, June 1991b (SECRET).

Petro, A.J., and D.L. Talent, "Removal of Orbital Debris," p. 169 ff. in *Orbital Debris from Upper-Stage Breakup*, J.P. Loftus, Ed., Vol. 121 in *Progress in Astronautics and Aeronautics*, AIAA, 1989.

Rees, D., Ed., *COSPAR International Reference Atmosphere: 1986, Part 1, Thermosphere Models* [CIRA-86], Pergamon Press, Oxford, 1989, p. 315 ff.

Scorer, R.S., *Environmental Aerodynamics*, Ellis Horwood, 1978.

Turner, R.E., and C.K. Hill, *Terrestrial Environment (Climatic) Criteria Guidelines for Use in Aerospace Vehicle Development*, 1982 Revision, NASA Tech. Memo. 82473, 1982.

U.S.A.F./A.R.D.C. *Handbook of Geophysics*, MacMillan, New York, Rev. Ed., 1960.

U.S. 1966 Standard Atmosphere Supplements, ESSA/NASA/USAF.

U.S. 1976 Standard Atmosphere, NOAA/NASA/USAF.

Valley, S.L., Ed., *Handbook of Geophysics and Space Environments*, USAF, 1965 (for US-62 Atmosphere, see p. 2-19 ff.).

Wallace, J.M., and P.V. Hobbs, *Atmospheric Science: an introductory survey*, Academic Press, 1977.

WGS-84, *DOD World Geodetic System 1984*, Defense Mapping Agency Report, TR 8350.2, September 1987.

APPENDIX A

ATMOSPHERIC VARIABILITY

APPENDIX A
ATMOSPHERIC VARIABILITY

APPENDIX A-1 LONG-TERM EFFECTS

These are selected figures from the U.S. 1966 Standard Atmosphere Supplements (to the US-62 Standard--denoted here by "66S") and from the U.S. 1976 Standard Atmosphere (cited in the captions here as "US-76"). They indicate the variability of atmospheric densities (Figs. A.1 to A.7) and temperatures (Figs. A.8 and A.9) with altitude, solar activity, time of day, latitude, and season. The reason for presenting this collection of figures is that they show the wide range of the parametric effects. Note that frequently the variability increases with increasing altitude.

The current NASA MSIS-90 atmosphere (Hedin, 1991) is available on computer tape, so that it exhibits a range of variability which is presumably comparable with that shown here.

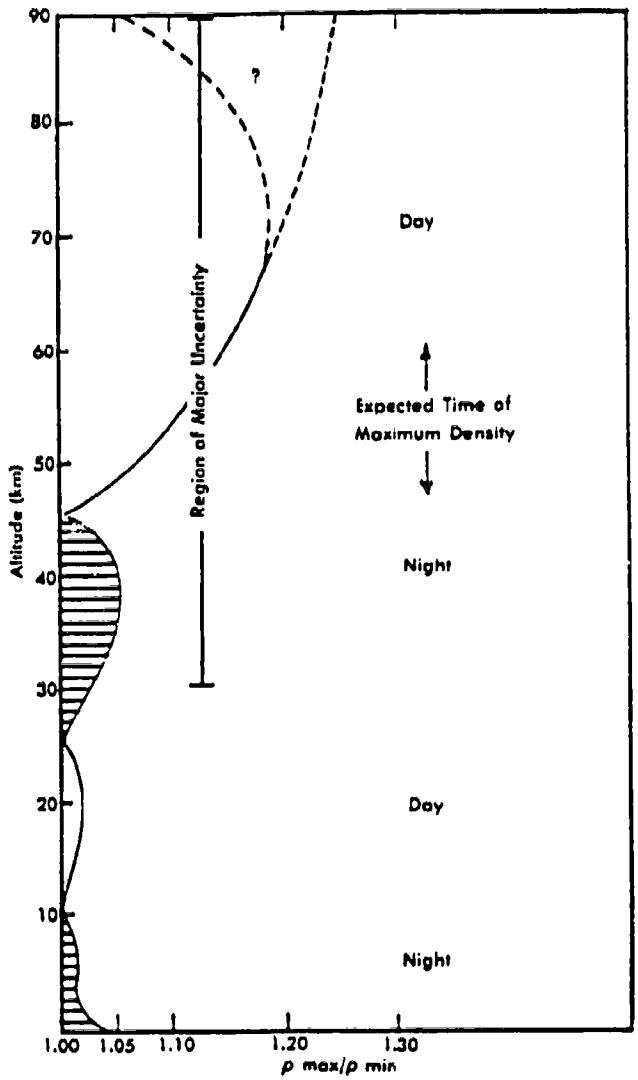

Figure A.1. Approximate Values of Diurnal Density Variability up to 90 km (66S--Fig. 2.12--see also Fig. 4 in the text for short-term variations)

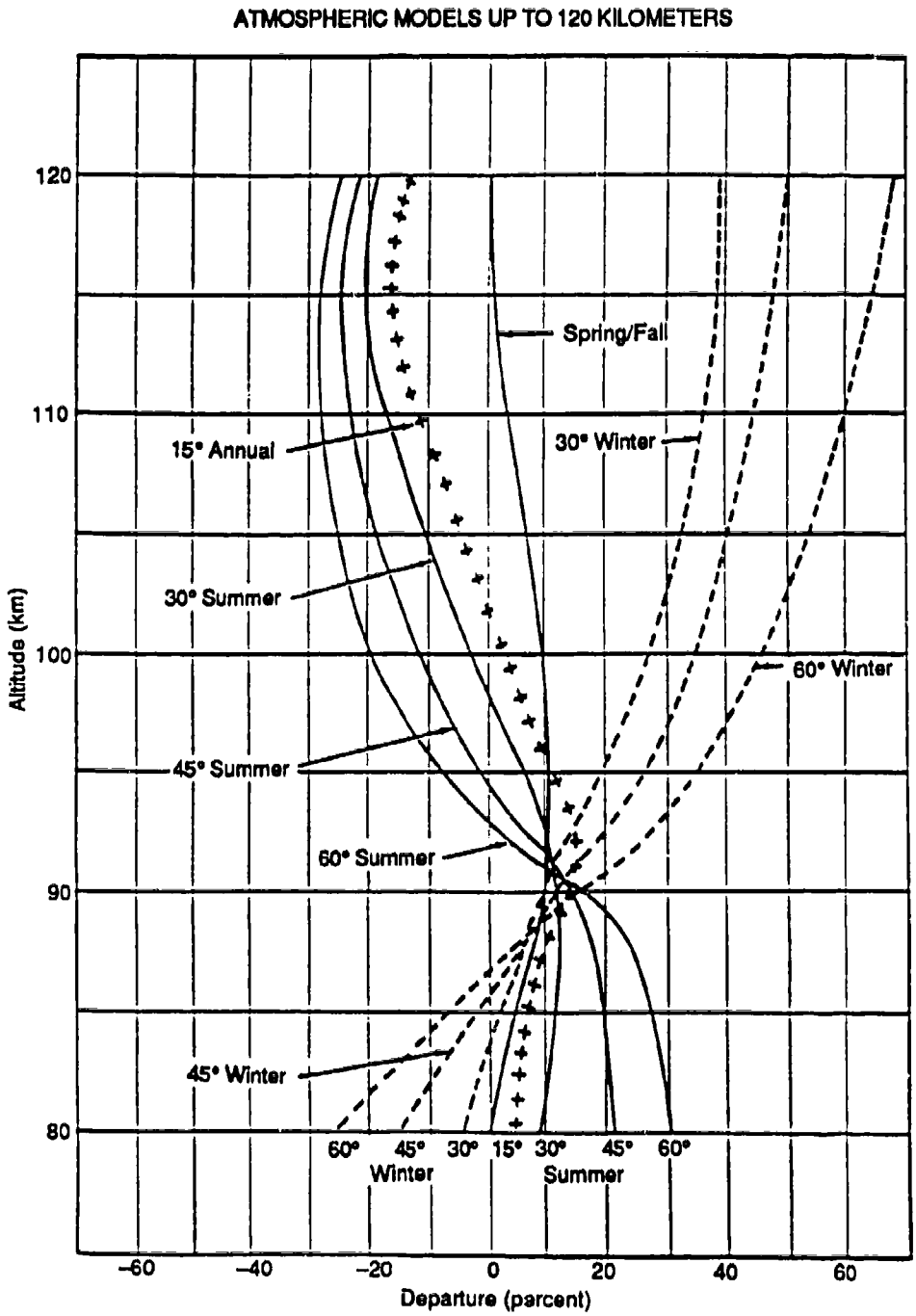

Figure A.2. Mean Density Variations With Latitude and Season, 80 to 120 km (66S--Fig. 2.6)

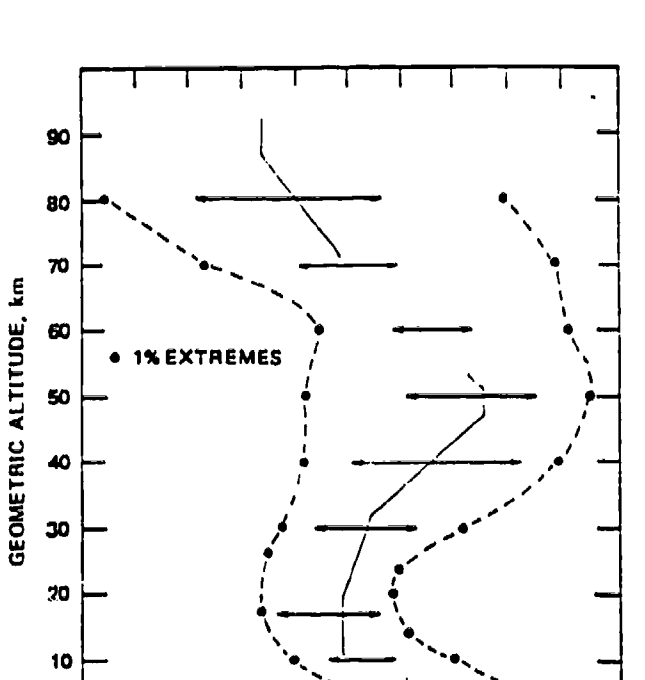

Figure A.3. Range of Systematic Variability of Temperature Around the U.S. Standard Atmosphere, 1976 (US76--Fig. 25)

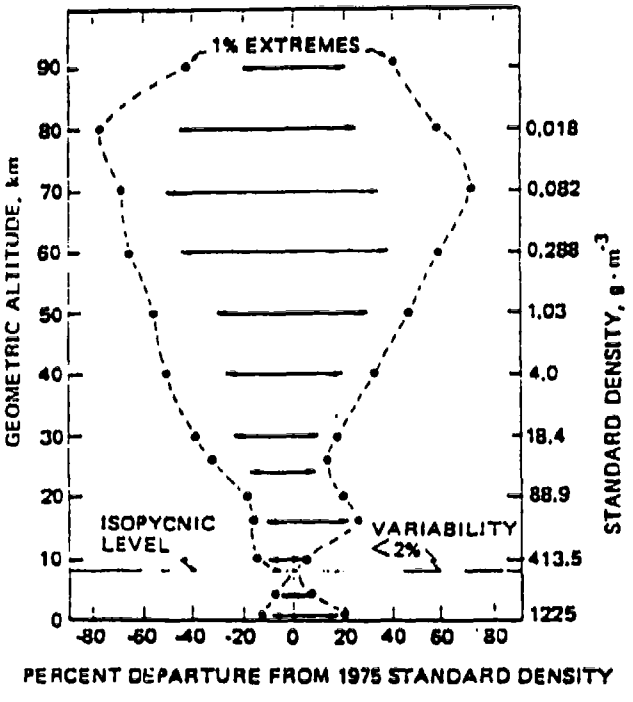

Above 30 km the largest deviations are in the Arctic and subArctic--negative in winter, positive in summer.

←—→ Includes season and latitudinal variation of mean monthly densities.

o - - - o 1 percent maximum/minimum densities that occur during months with high/low values in most extreme locations.

Figure A.4. Range of Systematic Variability of Density Around the U.S. Standard Atmosphere, 1976 (US76--Fig. 26)

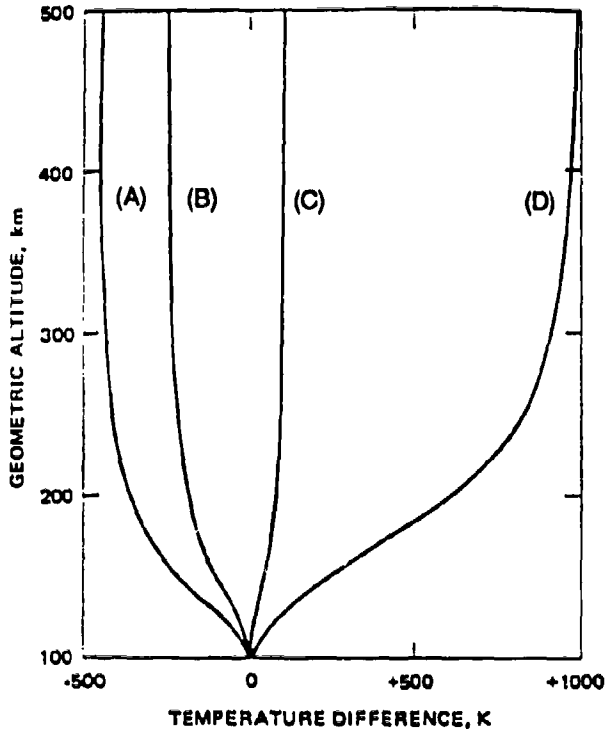

Figure A.5. Departures of the Temperature-Altitude Profiles From That of the US-76 Model for Various Degrees of Solar Activity (US76--Fig.28)

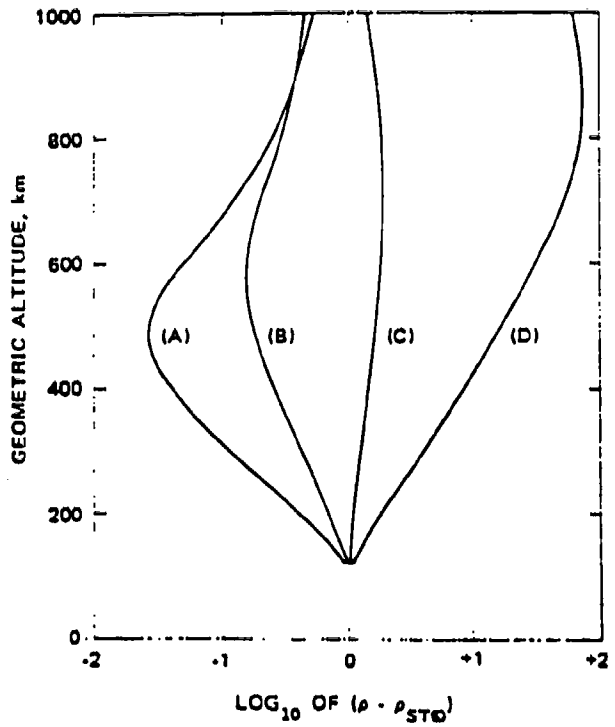

Figure A.6. Departures of the Density-Altitude Profiles From That of the US-76 Model for Various Degrees of Solar Activity (US76--Fig. 30)

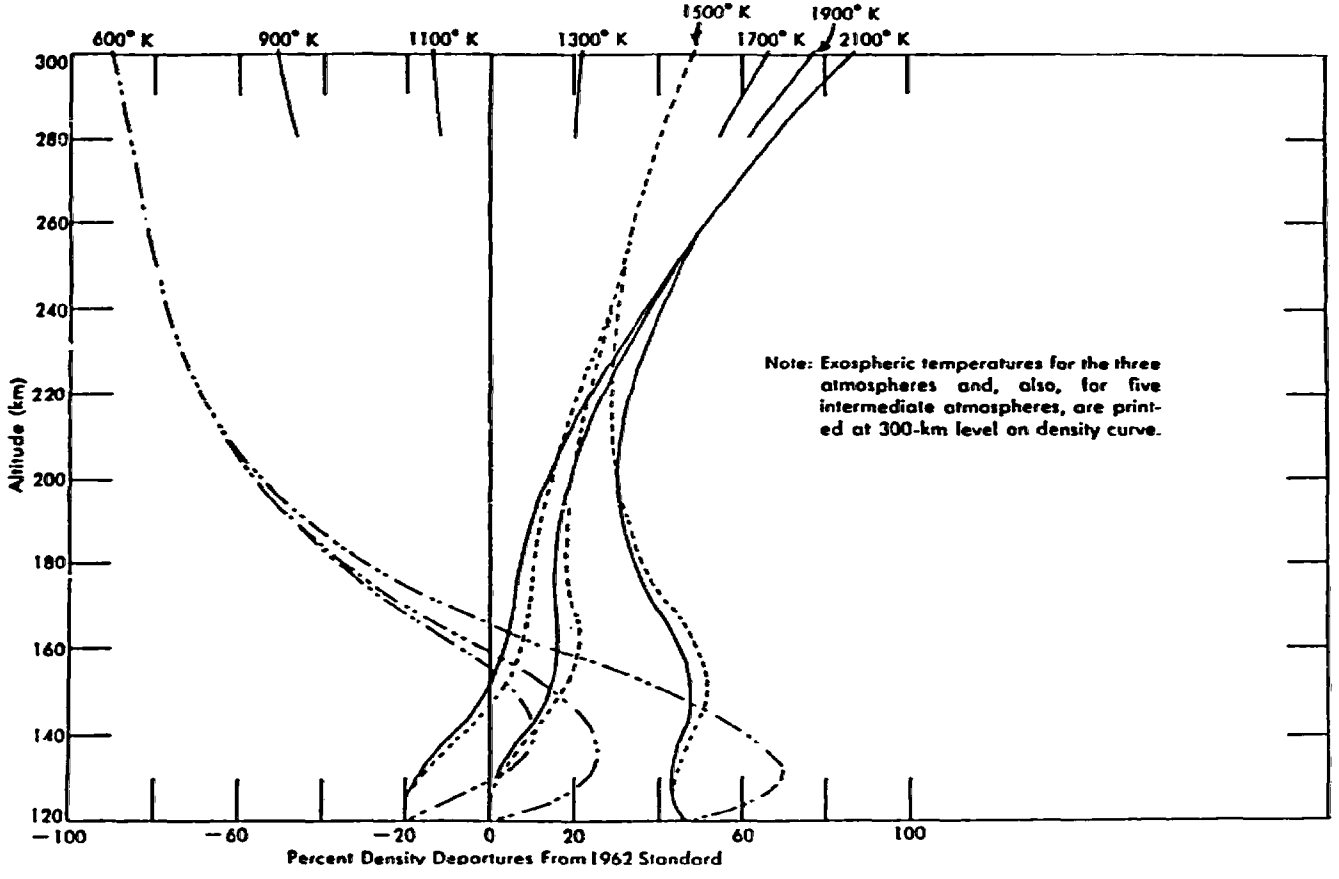

Figure A.7. Departures from the US-62 Standard of Densities for Summer, Winter, and Spring/Fall Models With Three Exospheric Temperatures (66S--Fig. 3.3)

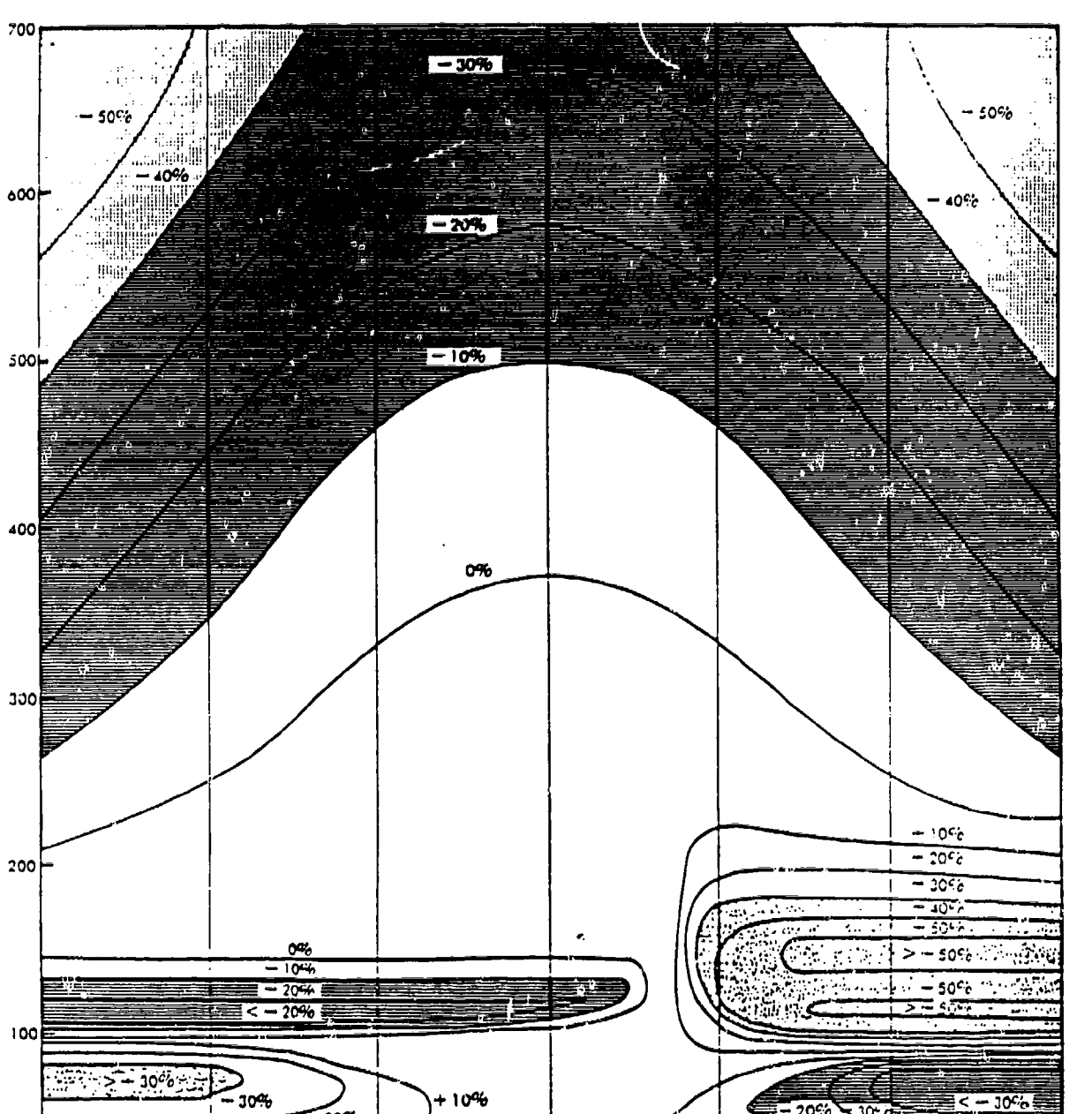

Figure A.8. Contours of Percentage Departures of Density from the US-62 Standard at All Latitudes Corresponding to 1400 Hours Local Time at Northern Hemisphere Summer Solstice With an Equatorial Bulge and a Maximum Exospheric Temperature of 1200 K (66S--Fig. 3.4)

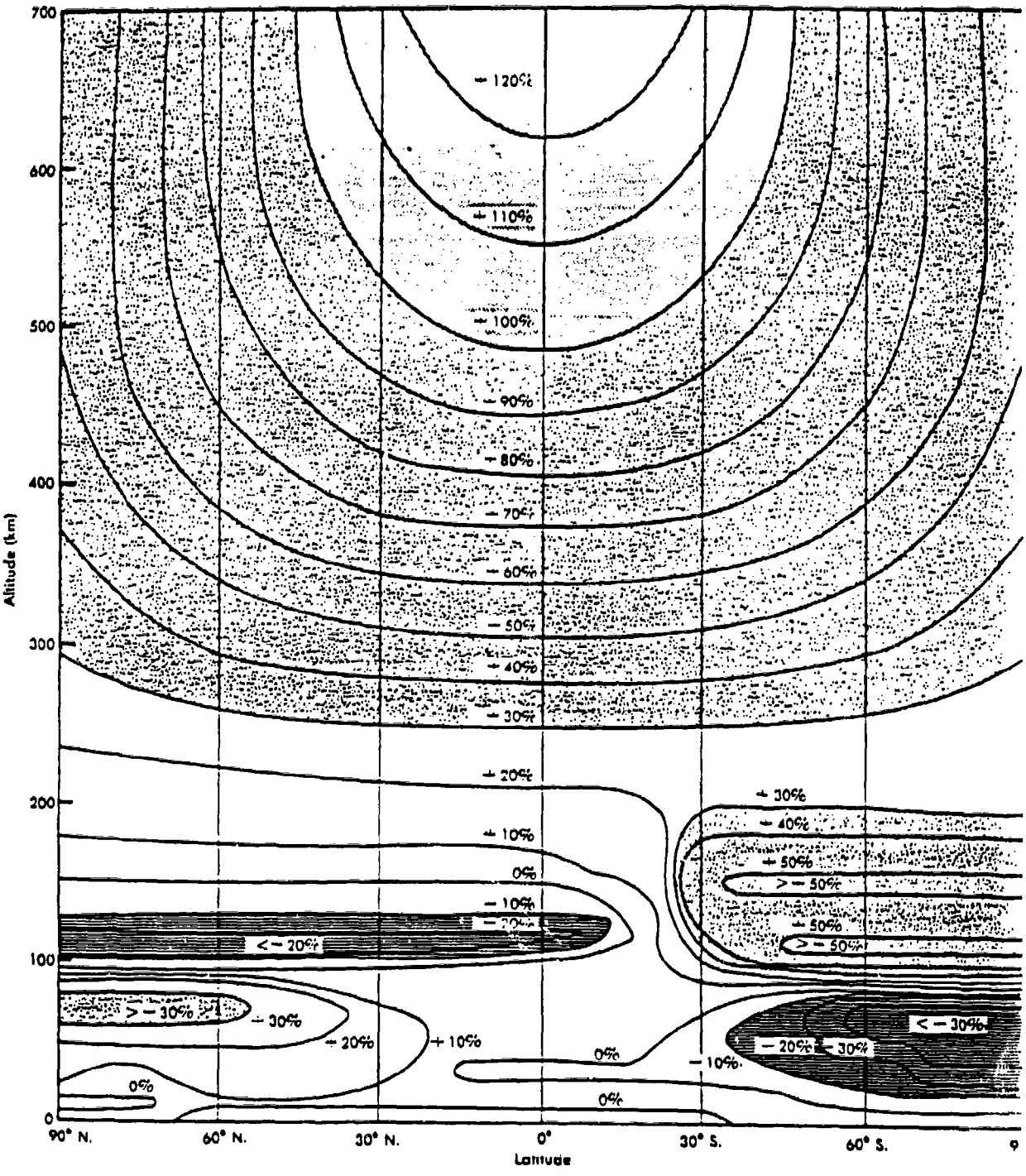

Figure A.9. Contours of Percentage Departures of Density From the US-62 Standard at All Latitudes Corresponding to 1400 Hours Local Time at Northern Hemisphere Summer Solstice With an Equatorial Bulge and a Maximum Exospheric Temperature of 1500 K (66S--Fig. 3.7)

APPENDIX A-2 SHORT-TERM ATMOSPHERIC DENSITY VARIATIONS

This discussion--based largely on Humphrey et al., 1981--expands on and explains Table 4 in the text.

Atmospheric tidal effects arise mainly from the thermal expansion of the atmosphere due to diurnal solar heating.[1] Figure A.10 (Humphrey et al., p. 83) shows tidal effects, which are significant mainly at the higher altitudes where the ambient atmospheric density is very low and the effect peaks near 2 p.m. local time.

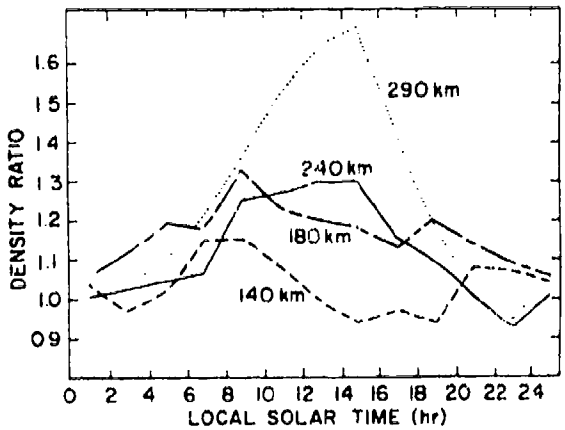

Figure A.10. Tidal Waves: Average Value of Measured Density to Jacchia (1971) Model Prediction as Function of Local Solar Time. The local time parameter for the model is taken to be local midnight in all cases, but all other parameters are handled in the manner prescribed in the model formulation. The data are binned at two-h intervals. Each curve includes all altitude increments within the 20 km band centered on the designated altitude. (Humphrey et al., 1981, p. 83)

Regarding Acoustic Gravity Waves (AGWs), there is a variety of short-term disturbances in the troposphere (below 8-16 km) which are amplified in going upward because conservation of momentum can be expressed as

$$\rho u^2 = \text{constant} \qquad (A.1)$$

where u = velocity; as density ρ falls off with increasing altitude, the velocity or magnitude of the effect increases. For a discussion of short-term disturbances in the troposphere, see,

---

[1] The physics is analogous to "nuclear heave" discussed in Section 2.6.

e.g., McIlveen, 1986, Ch. 11, and Wallace and Hobbs, 1977, p. 437 ff. Figure A.11 (Humphrey et al., p. 87) shows some "representative" upper atmospheric density measurements indicating how the amplitude of the effect increases with altitude, and Fig. A.12 gives measured scale sizes for AGWs and tidal waves.

Finally, let me explain where the word "gravity" comes from. If a parcel of air is displaced vertically and released in a convectively stable atmospheric layer,[2] then it oscillates about the level of neutral buoyancy with the Brunt-Vaisala frequency $N/2\pi$ which derived as follows. Consider a sample of air in an adiabatic balloon which is displaced from altitude z to $z + \delta z$ where the density is $\rho(z+\delta z)$. Thus the balloon experiences a buoyant force

$$g[(\delta\rho)_{outside} - (\delta\rho)_{inside}] = g.\delta z\,[d\rho/dz + \rho g/c^2] = -\rho\, N^2\, \delta z \qquad (A.2)$$

where

$$N^2 = -g\,[(1/\rho)\, d\rho/dz + g/c^2] \qquad (A.3)$$

N is the (Brunt-Vaisala frequency); representative values of the Brunt-Vaisala period 2p/N are 1-5 minutes.

Note that this kind of motion is one of a variety of mechanisms leading to atmospheric waves. Another mechanism is provided by the Kelvin-Helmholtz instability associated with a strongly sheared layer.[3] For more discussion of this whole field, see, e.g., Eckart, 1960; Hines, 1974; McIlveen, 1986; and Scorer, 1978.

---

2 In the troposphere the temperature normally decreases with increasing height. If the rate of fall-off of temperature with height is greater than the adiabatic lapse rate Γ_d, a parcel of air will be *stable*, whereas if the rate of falloff is smaller, the air parcel will not return to its initial position, i.e., will be *unstable*. Γ_d is 9.8C/km in dry air or ca 5C/km in saturated moist air.

3 Such an instability is demonstrated by the flapping of a flag in a breeze.

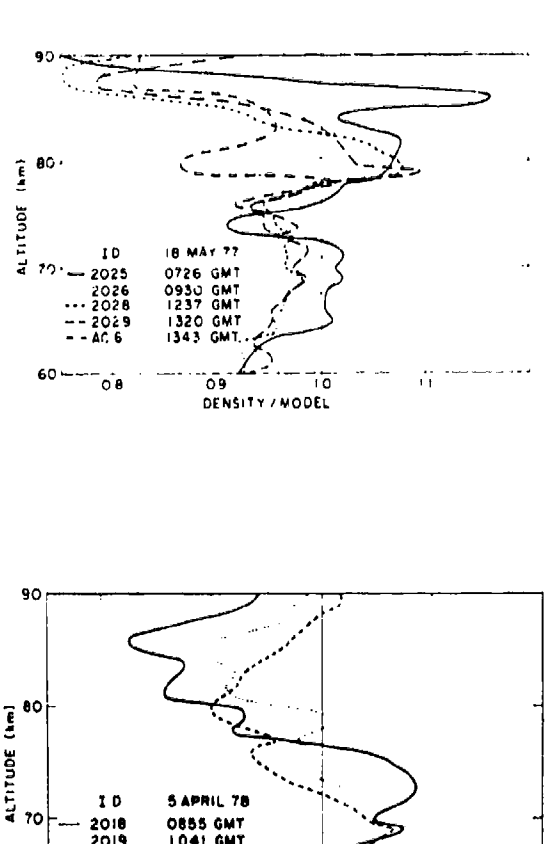

Figure A.11. Density Measurements from Falling Sphere Flights at Kwajalein. The density measurements are shown as a ratio to the Cole and Kantor tropical atmosphere for four Robin sphere flights and one accelerometer instrumented sphere (AC-6). (Humphrey et al., 1981, p. 87).

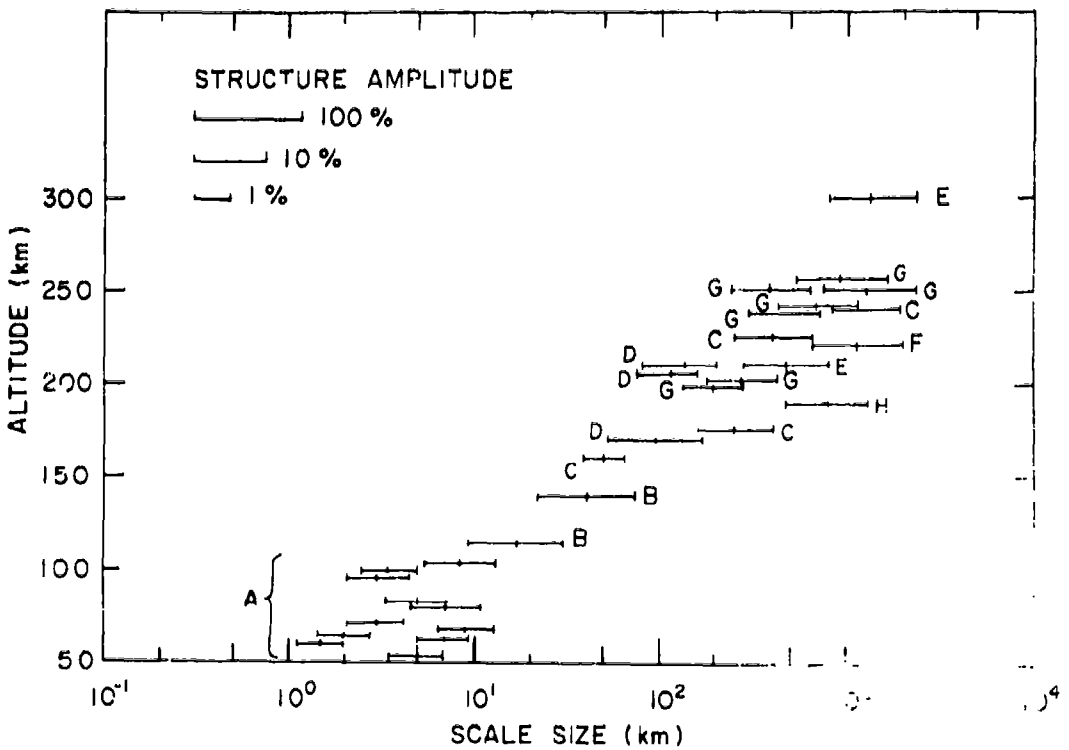

A. Rocketborne accelerometer, Philbrick et al, 1978a[47]
B. Rocketborne mass spectrometer, Trinks et al, 1978b[46]
C. AE-C satellite mass spectrometer, Reber et al, 1975[43]
D. AE-C satellite mass spectrometer, Potter et al, 1976[44]
E. S3-1 satellite mass spectrometer, Philbrick, 1976[48]
F. S3-1 satellite mass spectrometer, Trinks et al, 1978a[45]
G. S3-4 satellite density gauge, McIssac, 1979[42]
H. S3-1 satellite mass spectrometer, Philbrick, 1980[49]

Figure A.12. Altitude Distribution of Measured Scale Sizes for Atmospheric Waves. The rocketborne data show vertical structure and the satellite shows horizontal structure (Humphrey et al., 1981, p. 101, where the various listed references are cited).

APPENDIX B

ABSTRACT OF IDA PAPER P-506, *REENTRY VEHICLE DISPERSION DUE TO ATMOSPHERIC VARIATIONS*, Reinald G. Finke, August 1969 (Available through NTIS as AD 697 925)

APPENDIX B

ABSTRACT OF IDA PAPER P-506, *REENTRY VEHICLE DISPERSION DUE TO ATMOSPHERIC VARIATIONS*, Reinald G. Finke, August 1969 (Available through NTIS as AD 697 925)

Reentry vehicle impact displacements due to a fixed perturbation in density or in wind speed in each 5-km-thick layer of the atmosphere up to 90-km altitude have been derived from a series of machine reentry-trajectory calculations with the IDA Program RANGE for different R/Vs and reentry conditions. Three arbitrary reentry vehicle shapes were chosen whose ballistic coefficients (550, 1025, and 1975 lb/ft^2) were representative of the range of interesting values. Reentry conditions were varied, from those of IRBMs of 15,000 ft/sec at 50-deg path angle, to those for ICBMs of 22,500 ft/sec at 20-deg path angle, and reentry azimuths were varied from direct equatorial (tail wind) to retrograde equatorial (head wind). Intermediate reentry conditions were included to define the dependences well enough for interpolation, and even slight extrapolation, to all known interesting combinations.

The resulting layer-wide miss contributions from the most influential 5-km layers (centered at 5- and 10-km altitude) vary from about 200 ft for 1-percent change in density, or about 20 ft for 1-ft/sec change in wind speed for the low β and low reentry angle, to 0.4 ft for either 1-percent density change or 1 ft/sec of wind for the high β and high reentry angle.

At 60° N latitude, the worst-case, ~ 2σ density and wind departures from a monthly mean profile occur in January and amount to about 5 percent in density and 50 ft/sec in wind in the most influential 5- to 10-km-altitude range. The corresponding total miss distances due to the combined departures from the mean profile for all altitudes range from several thousand feet for the low β, low reentry angle down to several tens of feet for the high β, high reentry angle. These total miss distances vary as the minus 1.5 to 2 power of β, as the minus 1 power of reentry velocity, as the minus 3 to 5 power of the sine of the reentry angle, and negligibly with flight azimuth.

Allowable measurement errors for each layer to give a total impact uncertainty of 200 ft from combinations of all layers were derived. The minimum allowable errors in density and wind, occurring of course in the most influential 5- to 10-km layers, increase from the tightest extreme of about 0.1 percent and 1 ft/sec for low β, low reentry angle and combination as with common systematic error, to more than 50 percent and 200 ft/sec for high β, high reentry angle and combination as with random error.

APPENDIX C

CORRECTIONS FOR NONSPHERICITY OF THE EARTH

APPENDIX C
CORRECTIONS FOR NONSPHERICITY OF THE EARTH

The principal distortion of the earth from a sphere to an oblate spheroid is due to the long-term effect of the centrifugal Coriolis force arising from the earth's rotation. Over the time scale of the earth's lifetime, it has responded not as a rigid body but rather like a distortable fluid with a radius some 21 km greater at the equator than at the poles (cf., e.g., McIlveen, 1986, p.164 ff).

The effects of flattening of the earth on ballistic missile targeting are of the same order as the atmospheric effects considered here, some 20-40 km at ICBM ranges, and thus they should be included as appropriate.

As a result of the flattening and pear-shaped character of the earth, the gravitational potential for a satellite of mass m_1 distant r from the center of the earth is written as[1]

$$\Phi = (G\,M\,m_1/r)\,[1 + J_2/2r^2)\,(1 - 3\sin^2\delta) + (J_3/2r^3)\,(3 - 5\sin^2\delta)\sin\delta - (J_4/8r^4)\,(3 - 30\sin^2\delta + 35\sin^4\delta) - J_5 \ldots.\,]$$

where

G = gravitational constant

M = mass of earth

δ = geocentri. declination

J_2 J_3, J_4,... are the coefficients of the higher zonal harmonics.

Values for these coefficients currently (1992) used at the National Test Facility (NTF) are[2]

$J_2 = 1082.63 \times 10^{-6}$

$J_3 = -2.532 \times 10^{-6}$

$J_4 = -1.611 \times 10^{-6}$.

---

1 Cf. Koelle, 1961, p. 4-30.

2 NTF uses these coefficients to 9 significant figures.

Various numerical models for the nonsphericity of the earth are used. The current best model is WGS-84, but simplifications such as

- SGP--J_2, sun, moon, J_3, J_4
- The more detailed GP4 general perturbation
- SALT--semianalytical Liu theory

may be adequate for the current SDS applications.

APPENDIX D

ORBITAL DECAY RATES OF A GIVEN SATELLITE UNDER VARIOUS LEVELS OF SOLAR ACTIVITY

APPENDIX D
ORBITAL DECAY RATES OF A GIVEN SATELLITE UNDER VARIOUS LEVELS OF SOLAR ACTIVITY

Consider a satellite of mass W and average density ρ which is treated as a sphere of radius r so that its projected area A is

$$A = \pi r^2 = \pi(3W/4\pi\rho)^{2/3} \quad . \tag{D.1}$$

We introduce the drag coefficient C_D[1] and the ballistic coefficient β[2]

$$\beta = W/C_D A \tag{D.2}$$

which provides a measure for the total drag on the satellite.

For a circular orbit of radius $a = R_e + z$, where R_e = radius of earth = 6378 km, and z = altitude,

$$\Delta a \text{ per rev} = \Delta z \text{ per rev} = 2\pi a^2 \rho_o /(W/C_D A) \tag{D.3}$$

where ρ_o is the atmospheric density at altitude z.

Figure D-1 shows the variation of decay time with altitude for a cylindrical object 6.4 m in height, 2.4 m in diameter, and 350 kg mass as quoted by Petro and Talent, 1989. The lifetime of this satellite in a circular orbit at 400-km altitude is approximately 0.22 yr.

Note that in Eq. (D.3), $\Delta z \propto$ ambient density ρ_o / mass W ; thus assuming the same model atmosphere as in Fig. D-1 and the satellite parameters W = 50 kg, $C_D = 2$ and $A = 0.16\ m^2$, gives a lifetime of 3.0 yr for the same (400 km circular) orbit. Regarding the variation with atmospheric density, two plausible limits for ambient density at 400 km corresponding to solar minimum, i.e., low exospheric temperature and small high-altitude density, and to solar maximum, which corresponds to high exospheric temperature and

---

1 $C_D = 2$ for a flat plate normal to the flow, and $C_D = 2 \sin^2\theta$ for a cone of half-angle θ.

2 β is normally measured in lb/ft^2; 2000 lb/ft^2 = 9774 kg/m^2 is a representative value for the present generation of ablatively cooled reentry vehicles. (For a satellite, values of 50-200 kg/m^2 are typical, giving rise to life times of order several years in 400-500-km orbits.)

large high-altitude density, are given by Banks and Kockarts, 1973, as 9.0×10^{-16} g/cm^3 for solar min ($T_{exo} = 750$ K) and 1.1×10^{-14} g/cm^3 for solar max ($T_{exo} = 1500$ K).[3]

Thus, scaling with density, the mean lifetime of a given satellite in a circular orbit of height z = 400 km varies by a factor of 12 between solar minimum and solar maximum without propulsive cancellation of drag; this factor will of course vary with altitude. The lifetime of a satellite increases very much with increasing altitude. Thus at z = 1500 km the mean lifetime of the cylindrical satellite of Fig. D-1 will be of order 5000 yr, with a variation by a factor 2 between solar minimum and solar maximum.[4]

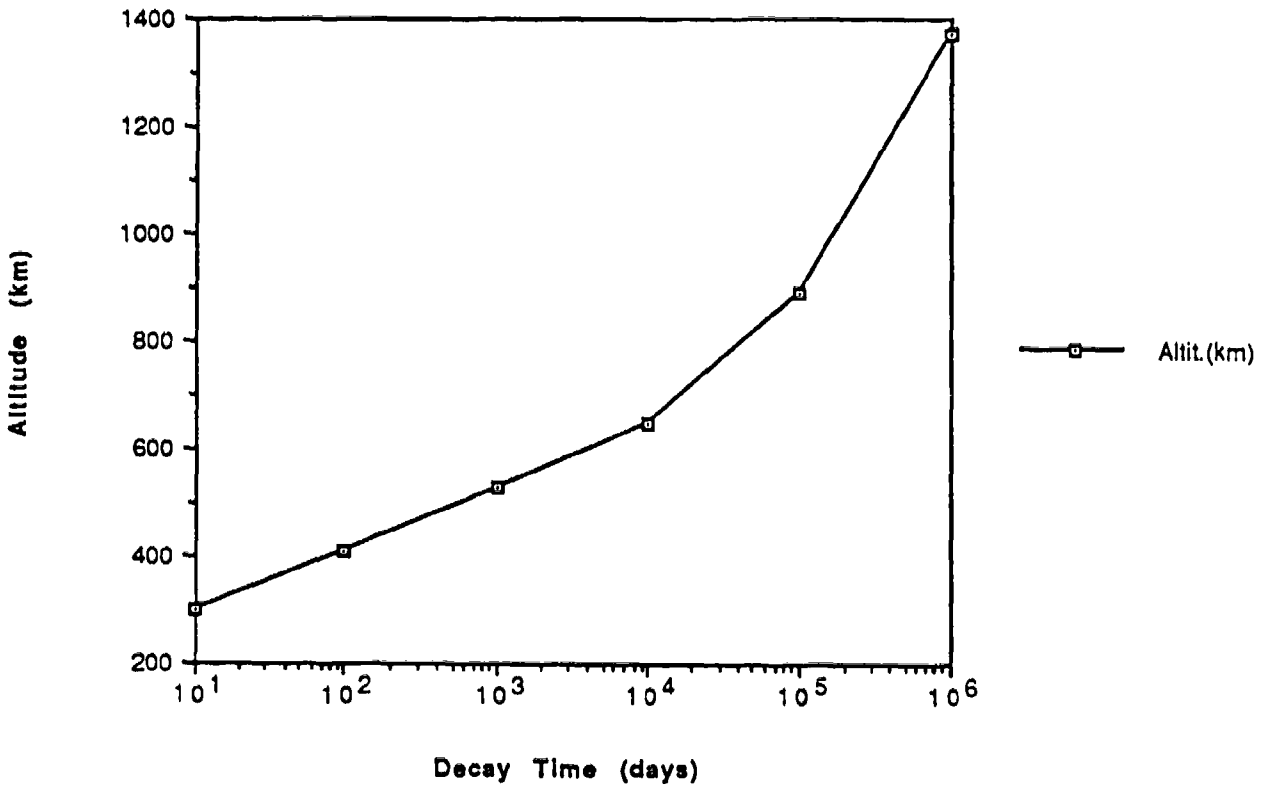

Figure D-1. Decay Time vs. Initial Altitude for a Cylindrical Satellite of 6.4 m Height and 2.4 m Diameter, and 350 kg Mass. (Petro and Talent, 1989, Jacchia -71 Model Atmosphere)

---

3 The U.S. Standard Atmospheres US-76 (low solar activity) and US-62 (high solar activity) give 2.8×10^{-15} and 6.5×10^{-15} gm/cm^3, respectively, for the density at 400 km.

4 For the spherical satellite of mass 50 kg and drag area A = 0.16 m^2 the mean lifetime at 1500 km is ~ 40,000 yr.

APPENDIX E

FSU (FORMER SOVIET UNION) STANDARD ATMOSPHERE

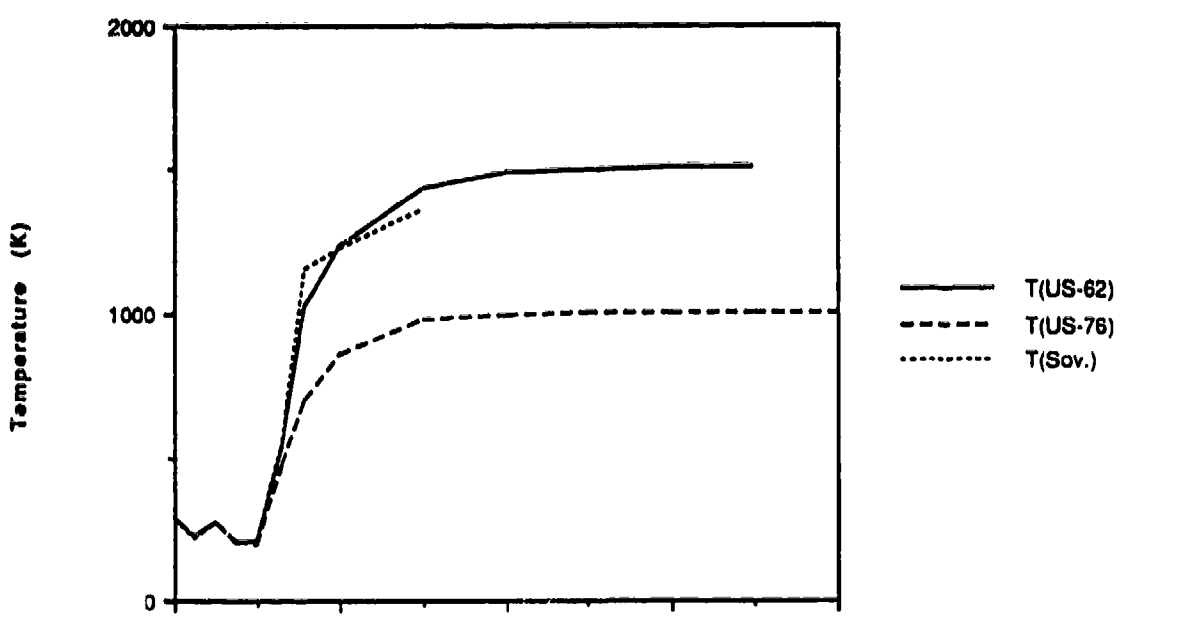

a. Temperature

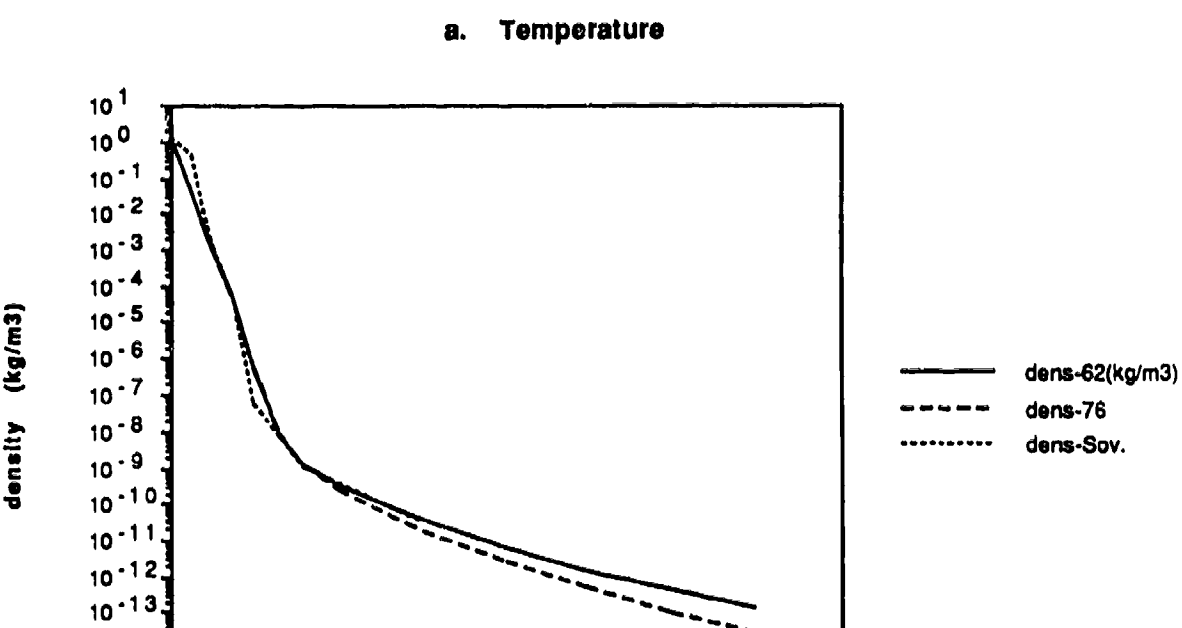

Note that below ca. 150 km the densities of the US-62 and US-76 model atmospheres coincide.

b. Density

Figure E-1. Atmospheric Temperature and Density from Former Soviet Standard Atmosphere compared with US-62 and US-76 Models

Table E-1. Standard Atmosphere (shortened)
(Source: V.I. Feodos'yev, Basic Technology of Rocket Flight, Moscow, Nauka, 1981) (In Russian)

h, m	p/p₀	ρ/ρ₀	T, K	h, m	p/p₀	ρ/ρ₀	T, K
−400	1,018	1,039	290,8	9 400	0,286	0,363	227,0
−200	1,021	1,019	289,5	9 600	0,278	0,355	225,7
0	1,000	1,000	288,2	9 800	0,270	0,348	224,4
200	0,976	0,981	286,9	10 000	0,261	0,338	223,1
400	0,954	0,962	285,6	10 200	0,254	0,329	221,8
600	0,931	0,944	284,2	10 400	0,246	0,321	220,6
800	0,909	0,925	282,9	10 600	0,238	0,313	219,2
1 000	0,887	0,908	281,6	10 800	0,231	0,306	218,0
1 200	0,866	0,890	280,3	11 000	0,224	0,298	216,7
1 400	0,845	0,872	279,0	11 200	0,217	0,289	216,7
1 600	0,824	0,855	277,7	11 400	0,210	0,280	216,7
1 800	0,801	0,838	276,4	11 600	0,204	0,271	216,7
2 000	0,781	0,822	275,1	11 800	0,197	0,263	216,7
2 200	0,765	0,805	273,8	12 000	0,191	0,255	216,7
2 400	0,746	0,789	272,5	12 200	0,185	0,247	216,7
2 600	0,728	0,773	271,2	12 400	0,180	0,239	216,7
2 800	0,710	0,758	269,9	12 600	0,174	0,232	216,7
3 000	0,692	0,742	268,6	12 800	0,169	0,221	216,7
3 200	0,675	0,727	267,3	13 000	0,161	0,218	216,7
3 400	0,658	0,712	266,0	13 200	0,159	0,211	216,7
3 600	0,641	0,698	264,7	13 400	0,151	0,204	216,7
3 800	0,624	0,683	263,4	13 600	$1,488 \cdot 10^{-1}$	0,198	216,7
4 000	0,609	0,669	262,1	13 800	1,412	0,192	216,7
4 200	0,593	0,655	260,8	14 000	1,398	0,186	216,7
4 400	0,577	0,641	259,5	14 200	1,355	0,180	216,7
4 600	0,562	0,628	258,2	14 400	1,313	0,175	216,7
4 800	0,548	0,614	256,9	14 600	1,272	0,169	216,7
5 000	0,533	0,601	255,6	14 800	1,233	0,164	216,7
5 200	0,519	0,588	254,3	15 000	1,195	0,159	216,7
5 400	0,505	0,576	253,0	15 200	1,158	0,154	216,7
5 600	0,492	0,563	251,7	15 400	1,122	$1,492 \cdot 10^{-1}$	216,7
5 800	0,479	0,551	250,4	15 600	1,087	1,446	216,7
6 000	0,466	0,539	249,1	15 800	1,054	1,401	216,7
6 200	0,453	0,527	247,8	16 000	1,021	1,358	216,7
6 400	0,441	0,515	246,5	16 200	0,990	1,316	216,7
6 600	0,429	0,504	245,2	16 400	0,959	1,276	216,7
6 800	0,417	0,493	243,9	16 600	0,930	1,236	216,7
7 000	0,406	0,482	242,6	16 800	0,901	1,199	216,7
7 200	0,394	0,471	241,3	17 000	0,873	1,161	216,7
7 400	0,383	0,460	240,0	17 200	0,846	1,125	216,7
7 600	0,373	0,450	238,7	17 400	0,820	1,091	216,7
7 800	0,362	0,439	237,4	17 600	0,795	1,057	216,7
8 000	0,352	0,429	236,1	17 800	0,770	1,031	216,7
8 200	0,342	0,419	234,8	18 000	0,746	0,993	216,7
8 400	0,332	0,410	233,5	19 000	0,638	0,849	216,7
8 600	0,322	0,400	232,2	20 000	0,545	0,725	216,7
8 800	0,313	0,391	230,9	21 000	0,466	0,620	216,7
9 000	0,304	0,381	229,6	22 000	0,399	0,530	216,7
9 200	0,295	0,372	228,3	23 000	0,341	0,453	216,7

h, m	p/p₀	ρ/ρ₀	T, K	h, m	p/p₀	ρ/ρ₀	T, K
24 000	0,292	0,388	216,7	65 000	$1,201 \cdot 10^{-2}$	$1,461 \cdot 10^{-2}$	236,2
25 000	0,249	0,332	216,7	70 000	0,576	0,757	219,1
26 000	0,213	0,280	219,4	75 000	0,260	0,371	202,1
27 000	0,183	0,237	222,1	80 000	$1,090 \cdot 10^{-2}$	$1,713 \cdot 10^{-3}$	185,0
28 000	$1,574 \cdot 10^{-1}$	0,202	224,9	85 000	0,117	0,696	185,0
29 000	1,355	0,171	227,6	90 000	$1,820 \cdot 10^{-3}$	0,281	185,0
30 000	1,168	$1,461 \cdot 10^{-2}$	230,4	95 000	0,742	$1,157 \cdot 10^{-3}$	185,0
31 000	1,010	1,248	233,1	100 000	0,320	0,441	209,2
32 000	0,874	1,068	235,8	110 000	$0,772 \cdot 10^{-3}$	$0,864 \cdot 10^{-4}$	257,1
33 000	0,758	0,915	238,5	120 000	0,252	0,217	312,2
34 000	0,658	0,786	241,3	130 000	$1,191 \cdot 10^{-3}$	$0,613 \cdot 10^{-4}$	552,0
35 000	0,573	0,676	244,0	140 000	0,729	0,267	768,0
36 000	0,499	0,583	246,7	150 000	0,506	$1,413 \cdot 10^{-4}$	980,0
37 000	0,435	0,503	249,5	160 000	0,376	0,905	1155,0
38 000	0,380	0,435	252,2	170 000	0,288	0,676	1175,0
39 000	0,333	0,377	254,9	180 000	0,222	0,509	1193,0
40 000	0,292	0,327	257,7	190 000	0,172	0,386	1211,0
41 000	0,258	0,281	260,4	200 000	$1,315 \cdot 10^{-3}$	0,295	1227,0
42 000	0,225	0,247	263,1	210 000	1,058	0,226	1217,0
43 000	0,198	0,215	265,8	220 000	0,837	0,175	1261,0
44 000	0,175	0,188	268,6	230 000	0,666	$1,360 \cdot 10^{-4}$	1277,0
45 000	$1,511 \cdot 10^{-1}$	0,161	271,3	240 000	0,533	1,061	1291
46 000	1,361	$1,435 \cdot 10^{-2}$	274,0	250 000	0,429	0,838	1301
47 000	1,207	1,269	274,0	260 000	0,317	0,662	1316
48 000	1,067	1,122	274,0	270 000	0,283	0,526	1321
49 000	0,944	0,993	274,0	280 000	0,231	0,421	1310
50 000	0,835	0,878	274,0	290 000	0,190	0,338	1350
55 000	0,452	0,481	270,6	300 000	0,157	0,274	1358
60 000	0,238	0,271	253,4				